[19] and BDNF protein [20] were decreased after ischemic stroke and housing in an enriched environment. Nygren et al. reported that BDNF +/− mice, which express low levels of BDNF, showed better stroke recovery in an enriched environment than their wild-type counterparts [12]. On the other hand, Risedal et al. observed no significant change of BDNF mRNA between rats in an enriched environment and those in a standard environment in their experiments using a permanent occlusion model [15]. In our previous investigation, microarray analysis and real-time reverse transcription polymerase chain reaction (RT-PCR) revealed a significant decrease in expression of the BDNF gene in the contralateral cortex to ischemia in rats in 4-week enriched environment [16]. Generally, BDNF is a beneficial molecule for neurons and neurological functions, and there thus appears to be a discrepancy between the decreased BDNF and improved neurological functions in these studies. There are at least two possible explanations for this phenomenon. The first one is that BDNF may be down-regulated, since the functionally improved brain may no longer need elevated BDNF after 4-week enrichment. Another possibility is that BDNF itself is an exacerbating factor for neurological deficit, especially in the post-stroke state, and that an enriched environment may eliminate BDNF to avoid its potentially deleterious effects. To examine these hypotheses, it will be necessary to examine brain tissue at an earlier time point when functional recovery has not been completed. Furthermore, proBDNF, a precursor of the BDNF protein, must be investigated, since it negatively influences neurons [9]. Thus, the objective of the present study was to investigate the expression of BDNF in rats subjected to focal cerebral ischemia followed by housing for 2 weeks in an enriched environment by using RT-PCR, Western blotting, and immunohistochemical techniques.

Nine-week-old, male Sprague–Dawley rats were anesthetized by chloral hydrate and the right middle cerebral artery (MCA) was occluded intraluminally for 60 min with nylon monofilaments, as previously described [8]. At 72–96 h after transient MCA occlusion (tMCAO), the rats were randomly divided into two groups, an enriched group and a standard group. For the enriched group, 4–6 rats were housed together in a large cage (610 mm × 460 mm × 460 mm) containing toys including a running wheel, a tunnel, balls, logs and rings, rearranged twice a week. For the standard group, rats were housed alone in a standard-sized cage (320 mm × 210 mm × 130 mm) containing food and water.

Ischemic animals were subjected to two behavioral tests, the neurological severity score test (NSS) [2] and the inclined plane test (IPT) [6]. These tests were performed 3 times, once before tMCAO, once at 3 or 4 days after tMCAO (defined as day 0), and once at 14 days after initiation of differential housing (defined as day 14). The NSS is a composite of motor, sensory, reflex, and balance tests. The score ranges from 0 to 18, with the higher score indicating severe neurological impairment. In this study, we analyzed rats that scored between 7 and 12 in the second test (day 0). The recovery rate was defined as $(NSS_{2nd} - NSS_{3rd})/NSS_{2nd}$. The IPT was performed to evaluate motor deficits. Each rat was placed up-headed or right-headed on a stainless steel plane steepening at a rate of $2° s^{-1}$, and we recorded the angle when the rat slipped on the plate. The improvement index was calculated as $(IPT_{3rd} - IPT_{2nd})/(IPT_{1st} - IPT_{2nd})$. After the behavioral tests on day 14, rats were sacrificed and the brains were cut into 3 coronal sections with a thickness of 3 mm from the frontal pole.

The second blocks from the frontal pole were embedded in paraffin for the histological study. Microtubular-associated protein 2 (MAP-2), glial fibrillary acidic protein (GFAP), synaptophysin (SYP), and matBDNF were immunohistochemically stained. The infarct volume was calculated as $(C-I)/C$, where C represents MAP-2-stained volume in contralateral side, and I represents MAP-2-stained volume in ischemic side. To set regions of interest in peri-infarct area, we assessed both neuronal viability using MAP-2 staining and glial activity using GFAP staining. MAP-2 mainly distinguishes infarct area from non-infarct area, and GFAP mainly distinguishes peri-infarct area and distant intact area. The area with both preserved MAP-2 staining and intense GFAP staining was defined as peri-infarct area. SYP and BDNF immunoreactivity was quantified in peri-infarct area and its contralateral cortex. The rate of the positively stained area was compared between the two groups.

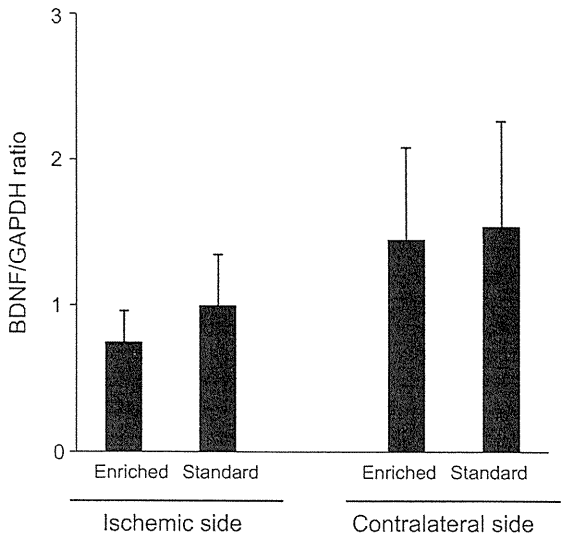

Fig. 1. BDNF gene expression showed no significant differences between the enriched and standard groups on the ischemic side ($p = 0.16$) or contralateral side ($p = 0.81$). Data were normalized to the ischemic side of the standard group.

The peri-infarct cortex and its contralateral cortex of the third blocks were subjected to real-time RT-PCR or Western blotting. Total RNA from the peri-infarct cortex and contralateral cortex was isolated and analyzed for gene expression by real-time quantitative RT-PCR. Expression levels of BDNF mRNA were normalized to those of GAPDH mRNA. For Western blotting, primary antibodies were HRP-conjugated anti-β actin antibody, anti-BDNF antibody, and anti-proBDNF antibody. The anti-proBDNF antibody was produced in a rabbit by intravenous injection of proBDNF-specific peptide. The secondary antibody was HRP-conjugated anti-rabbit goat IgG. The chemiluminescence agents were ECL or ECL+Plus (GE Healthcare). An LAS-4000miniEPUV (FUJIFILM) CCD camera was used to quantify the band intensity. As positive controls, recombinant human BDNF and C6 glioma cell lysate was applied for Western blotting.

Data are expressed as the means ± SD, and a p-value less than 0.05 was considered statistically significant. See the supplementary document for more information about the methods.

The neurological and motor functions of rats in both groups were impaired after t-MCAO and improved on day 14 (Table 1). A significant difference was observed in both NSS and IPT on day 14, but not on day 0, between the enriched ($n = 24$) and standard ($n = 22$) groups. The recovery rate for NSS and improvement index for IPT both indicated a significant improvement in function in the enriched group compared to the standard group.

The infarction area evaluated by immunoreactivity to MAP-2 in the enriched group (56.82 ± 7.31%, $n = 14$) was not significantly different from that in the standard group (55.44 ± 11.50%, $n = 13$, $p = 0.72$).

We performed real-time RT-PCR to examine the changes in BDNF levels (Fig. 1). The data presented were normalized to the ischemic side of the standard group. On the ischemic side, the BDNF/GAPDH ratio was 0.75 ± 0.21 ($n = 7$) in the enriched group, which was slightly but not significantly lower than that in the stan-

Table 1
Behavioral test results.

	Pre-MCAO		Day 0		Day 14	
	Enriched $n=24$	Standard $n=22$	Enriched	Standard	Enriched	Standard
NSS	0.00 ± 0.00	0.00 ± 0.00	8.00 ± 1.02	7.55 ± 0.74	4.92 ± 1.32*	5.73 ± 1.03
NSS recovery rate					37.83 ± 17.95*	23.67 ± 14.08
IPT up-headed	51.72 ± 2.00	50.80 ± 1.74	42.26 ± 2.61	43.52 ± 2.34	47.54 ± 1.63*	45.37 ± 2.30
IPT right-headed	50.60 ± 2.86	50.79 ± 2.62	41.63 ± 2.62	42.80 ± 2.94	47.08 ± 2.11*	45.61 ± 2.11
IPT mean	51.16 ± 2.16	50.79 ± 1.90	41.94 ± 2.39	43.16 ± 2.37	47.31 ± 1.70*	45.49 ± 2.15
IPT improvement index					59.17 ± 29.51*	27.75 ± 40.25

* $p<0.05$ compared to the standard group. Data are presented as the means ± SD.

dard group (1.00 ± 0.35, $n=6$). On the contralateral non-ischemic side, there was no significant difference in the BDNF/GAPDH ratio between the enriched group (1.45 ± 0.63, $n=8$) and standard group (1.54 ± 0.72, $n=6$).

Fig. 2 summarizes the results of Western blotting for matBDNF and proBDNF. The antibodies for matBDNF and proBDNF were validated with Western blotting using recombinant matBDNF and C6 glioma cell lysate, respectively (Fig. 2A). There were no significant differences between the enriched group ($n=8$) and standard group ($n=8$) in either matBDNF on the ischemic side (Fig. 2B), matBDNF on the contralateral side (Fig. 2C), proBDNF on the ischemic side (Fig. 2D), or proBDNF on the contralateral side (Fig. 2E), although the level of matBDNF in ischemic side tended to be slightly lower in the enriched group than in the contralateral group.

Fig. 3 shows the results of immunohistochemical staining of GFAP, SYP and BDNF. The areas stained with SYP and BDNF were quantified. The SYP-stained area on the ischemic side ($n=14$) was significantly increased in the enriched group ($n=13$) compared to the standard group (Fig. 3B, 2.57 ± 0.28% vs 2.07 ± 0.23%, $p<0.001$), although no significant difference was observed on the contralateral side (Fig. 3C, 1.56 ± 0.29% vs 1.49 ± 0.30%, $p=0.52$). On the other hand, the matBDNF-stained area on the ischemic side was slightly smaller in the enriched group ($n=15$) than in the standard group ($n=12$), although the difference did not reach the level of statistical significance (Fig. 3D). On the contralateral side, the enriched group showed a matBDNF-stained area comparable to that of the standard group without significant difference (Fig. 3E).

This study showed that housing in an enriched environment for 2 weeks significantly enhanced the functional recovery of rats after ischemic stroke. In addition, the immunohistochemical findings of increased SYP staining indicated an increased density of synapses. On the other hand, no significant difference was observed in the volume of infarction, mRNA expression of BDNF, or protein expressions of BDNFs.

Our previous investigation using a 4-week period of housing demonstrated a decrease in BDNF gene in the animals housed in an enriched environment based on microarray analysis and real-time RT-PCR as well as a continuous improvement of neurological functions until 4-week [16]. To further clarify the mechanisms of decreased BDNF expression, in the present study we measured the levels of the BDNF protein and gene after a shorter period of enriched environment, i.e., 2 weeks. The common finding between

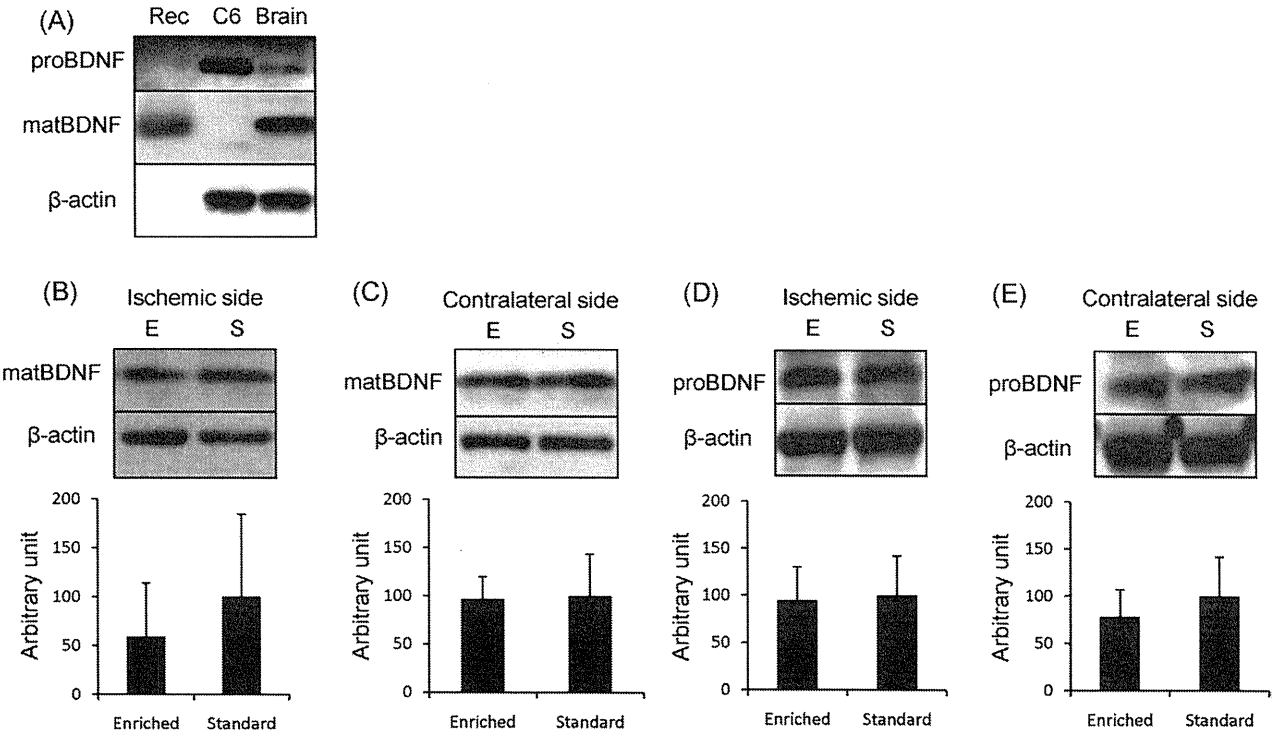

Fig. 2. Western blotting. (A) Recombinant human matBDNF (Rec), C6 glioma cell lysate (C6), and rat brain tissue validated the use of the antibodies for matBDNF (14 kDa) and proBDNF (32 kDa). Rat brain tissue contained detectable levels of these molecules. The levels of (B) matBDNF on the ischemic side ($p=0.27$), (C) matBDNF in contralateral side ($p=0.86$), (D) proBDNF on the ischemic side ($p=0.79$), and (E) proBDNF on the contralateral side ($p=0.25$) were not significantly different between the enriched and standard groups. Abbr. E: enriched group; S: standard group.

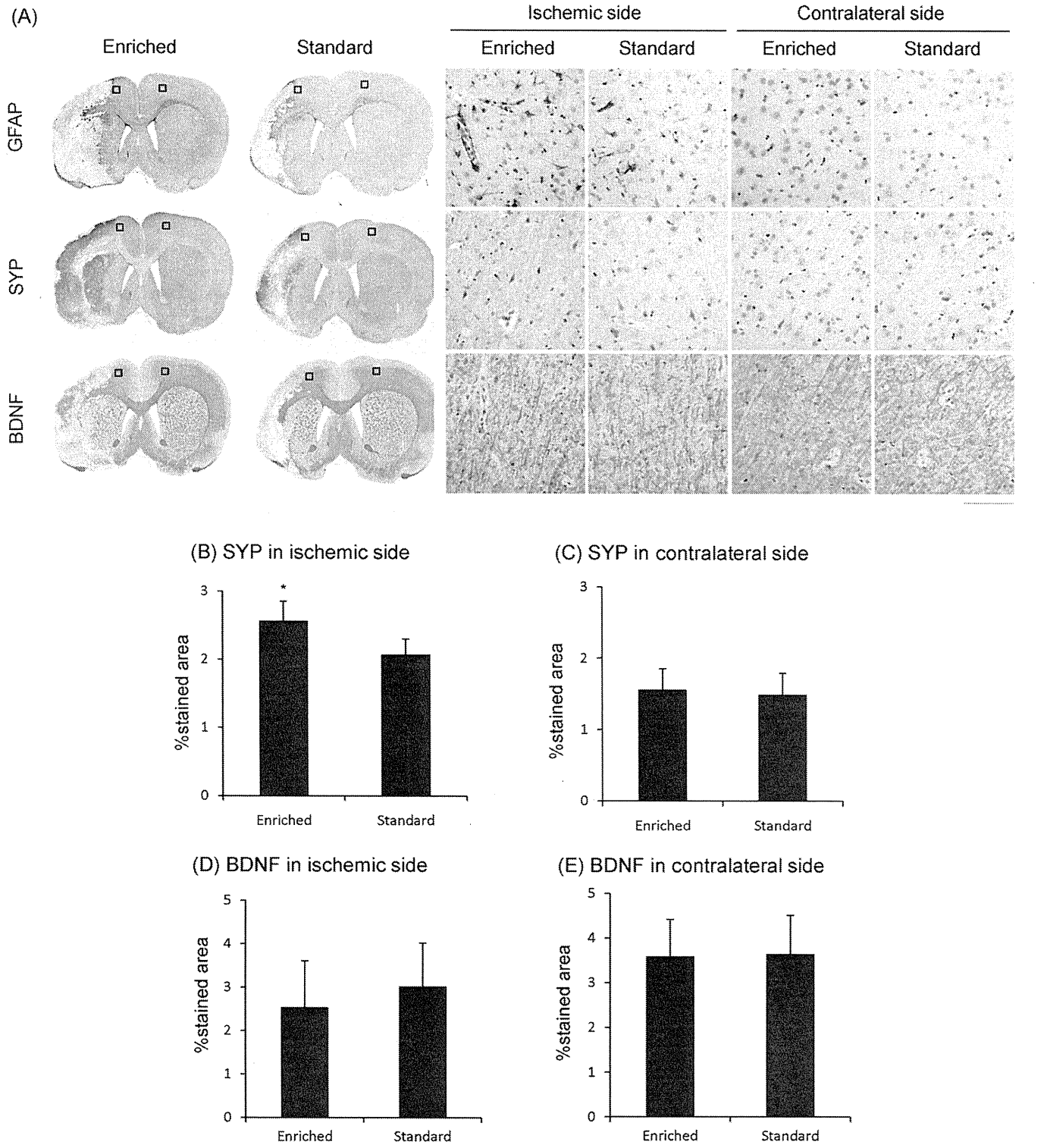

Fig. 3. Immunohistochemical analysis of GFAP, SYP, and matBDNF levels on the ischemic side and contralateral side. (A) Representative whole brain images (left 2 columns) and enlarged images (right 4 columns). The ischemic side was the left in the picture (right hemisphere of the rats). Squares indicate the enlarged sites. The bar represents 100 μm. (B–E) The SYP- and BDNF-stained areas were quantified. The ischemic side in the enriched group showed significantly stronger staining than the ischemic side in the standard group (B) ($p < 0.001$), while the contralateral side in the enriched group and contralateral side in the standard group did not show a significant difference (C) ($p = 0.52$). On the other hand, the matBDNF-stained area on the ischemic side (D) ($p = 0.24$) and contralateral side (E) ($p = 0.85$) showed no significant difference.

the 2-week and 4-week experiments was the lack of a clear increase in BDNF gene expression, despite the well-known beneficial effects of BDNF for neurons and neurological functions under various physiological and pathological conditions. These results, combined with our previous findings showing amelioration of neurological sign after 2 weeks, suggest that the functional recovery induced by an enriched environment might be brought about by mechanisms other than increased BDNF.

As an explanation for the relationship between BDNF and functional recovery, we hypothesized that proBDNF might play an

important role. The primary product of the BDNF gene is the 32-kDa proBDNF protein, which is translated in neurons and released into the extracellular space. Proteolytic enzymes such as plasmin cleave proBDNF into 14-kDa matBDNF and another particle. While matBDNF binds to the TrkB receptor on neurons and induces cell survival, differentiation, and long-term potentiation, proBDNF binds to the p75NTR receptor on neurons and induces apoptosis of neurons and long-term depression [9,11,17]. Thus, proBDNF and matBDNF, originating from the same gene, have opposite effects. Therefore, not only transcriptional regulation but also post-translational modification must be taken into consideration when we discuss the effects of BDNF. Via its pro-apoptotic effect, proBDNF might have an exacerbating effect on the ischemic damage of neurons and therefore neurological functions. If so, the decrease in proBDNF is beneficial. However, to our knowledge, there has been no studies investigating proBDNF expression in relation to stroke and enriched environment, although Zhao et al. previously measured the total levels of matBDNF and proBDNF using ELISA with anti-matBDNF antibody [20]. In the present work, we first tried to measure proBDNF using commercially available antibodies. Theoretically, Western blotting using either a proBDNF-specific antibody or matBDNF antibody could be used to quantify proBDNF levels, since the matBDNF domain is common to proBDNF and matBDNF. However, we did not find an efficient antibody that clearly revealed the band of proBDNF. Therefore, in the present study, we produced a polyclonal antibody using a proBDNF-specific peptide. Contrary to our expectations, Western blotting revealed no significant difference in proBDNF expression between the enriched group and standard group. This finding clearly indicates that the functional improvement induced by an enriched environment cannot be ascribed to decreased proBDNF.

On the other hand, an interesting difference between the 2-week and 4-week experiment is that a significant decrease in BDNF gene expression was observed after 4 weeks but not after 2 weeks of enrichment. Therefore, the difference in BDNF expression may be amplified between 2 weeks and 4 weeks. Considering that functional recovery and synaptogenesis were already observed at 2 weeks, there is a possibility that the decrease of BDNF expression at 4 weeks might result from secondary down-regulation due to the improved neurological functions. To prove the hypothesis, further investigation will be necessary to collect samples in earlier time points than 2 weeks, especially before the significant improvement becomes evident in enriched group. Not only BDNF gene expression but also matBDNF protein showed a consistent trend of decrease by both Western blotting and immunohistochemical staining, although the difference was not statistically significant. These results agree with the report by Zhao et al., which demonstrated a decrease in the total levels of BDNF protein in an enriched group [20]. Thus, we cannot completely rule out type-2 statistical error that small analyzing numbers concealed the possible decrease in BDNF genes or matBDNF in enriched group. Even if that is the case, however, there is no evidence of increase in BDNF genes or matBDNF.

Few genes are known to have a relationship to enriched housing environments. Dahlqvist et al. reported an alteration in the levels of nerve growth factor-induced gene A and glucocorticoid receptor following environmental enrichment in rats [4]. We previously found that animals in an enriched housing group showed a decrease in Early growth response-1 (Erg-1) mRNA [16], which is an inflammatory gene associated with exacerbation of neurological deficits after stroke [18]. To clarify the mechanisms of enriched environment-induced functional recovery, future investigations of neurotrophic factors other than BDNF (i.e., nerve growth factor, neurotrophin-3, and neurotrophin-4) and other inflammatory genes will be needed. Since the environmental stimulation involves a series of complicated processes through which many genes and proteins are expected to alter their expression, the combination of exhaustive analysis of the relevant genes and proteins will provide additional information.

We observed no decrease in infarction volume in the enriched group. This finding is consistent with previous reports [1,13]. Functional recovery induced by an enriched environment is not due to a reduction of infarct volume but possibly due to functional compensation in the brain tissues that escaped from infarction. The increased density of synapses in peri-infarct cortex measured using the SYP-stained area further supports this hypothesis.

One may argue that an enriched environment is a model enhancing voluntary exercise and thus the effect depends on individual activity, leading to a great individual variability in stroke recovery. However, as far as animal experiments are concerned, the effect of forced exercise such as treadmill running is controversial [7,10,14], while most studies on environmental enrichment agree on its positive effects. Therefore, we consider that enriched housing is a more feasible model to investigate the mechanisms of functional recovery after brain ischemia. Because it is established that environmental enrichment leads to an increase in BDNF in non-ischemic healthy animals [5], we compared only ischemic rats between enriched and standard environments according to the previous research designs [19,20].

In conclusion, an improvement of neurological functions was induced by an enriched environment accompanied with an increased density of synapses but without a reduction of infarct volume. The 2-week environmental enrichment did not significantly alter BDNF expression, including BDNF mRNA, matBDNF protein, or proBDNF protein. These results suggest that the functional recovery might not be due to increased BDNF or decreased proBDNF but rather to other underlying mechanisms.

Acknowledgements

This study was partially supported by Special Coordination Funds for Promoting Science and Technology of the Ministry of Education, Culture, Sports, Science and Technology of the Japanese Government. This research was also partially supported by a Grant-in-Aid for General Scientific Research from the Japan Society for the Promotion of Science.

Appendix A. Supplementary data

Supplementary data associated with this article can be found, in the online version, at doi:10.1016/j.neulet.2011.03.068.

References

[1] J. Biernaskie, D. Corbett, Enriched rehabilitative training promotes improved forelimb motor function and enhanced dendritic growth after focal ischemic injury, J. Neurosci. 21 (2001) 5272–5280.
[2] J. Chen, Y. Li, L. Wang, Z. Zhang, D. Lu, M. Lu, M. Chopp, Therapeutic benefit of intravenous administration of bone marrow stromal cells after cerebral ischemia in rats, Stroke 32 (2001) 1005–1011.
[3] S.C. Cramer, Repairing the human brain after stroke. I. Mechanisms of spontaneous recovery, Ann. Neurol. 63 (2008) 272–287.
[4] P. Dahlqvist, L. Zhao, I.M. Johansson, B. Mattsson, B.B. Johansson, J.R. Seckl, T. Olsson, Environmental enrichment alters nerve growth factor-induced gene A and glucocorticoid receptor messenger RNA expression after middle cerebral artery occlusion in rats, Neuroscience 93 (1999) 527–535.
[5] B.R. Ickes, T.M. Pham, L.A. Sanders, D.S. Albeck, A.H. Mohammed, A.C. Granholm, Long-term environmental enrichment leads to regional increases in neurotrophin levels in rat brain, Exp. Neurol. 164 (2000) 45–52.
[6] B.B. Johansson, A.L. Ohlsson, Environment, social interaction, and physical activity as determinants of functional outcome after cerebral infarction in the rat, Exp. Neurol. 139 (1996) 322–327.
[7] M.W. Kim, M.S. Bang, T.R. Han, Y.J. Ko, B.W. Yoon, J.H. Kim, L.M. Kang, K.M. Lee, M.H. Kim, Exercise increased BDNF and trkB in the contralateral hemisphere of the ischemic rat brain, Brain Res. 1052 (2005) 16–21.

[8] Y. Kuge, K. Minematsu, T. Yamaguchi, Y. Miyake, Nylon monofilament for intraluminal middle cerebral artery occlusion in rats, Stroke 26 (1995) 1655–1657 (discussion 1658).
[9] B. Lu, P.T. Pang, N.H. Woo, The yin and yang of neurotrophin action, Nat. Rev. Neurosci. 6 (2005) 603–614.
[10] A. Moraska, T. Deak, R.L. Spencer, D. Roth, M. Fleshner, Treadmill running produces both positive and negative physiological adaptations in Sprague–Dawley rats, Am. J. Physiol. Regul. Integr. Comp. Physiol. 279 (2000) R1321–R1329.
[11] S.J. Mowla, H.F. Farhadi, S. Pareek, J.K. Atwal, S.J. Morris, N.G. Seidah, R.A. Murphy, Biosynthesis and post-translational processing of the precursor to brain-derived neurotrophic factor, J. Biol. Chem. 276 (2001) 12660–12666.
[12] J. Nygren, M. Kokaia, T. Wieloch, Decreased expression of brain-derived neurotrophic factor in BDNF(+/−) mice is associated with enhanced recovery of motor performance and increased neuroblast number following experimental stroke, J. Neurosci. Res. 84 (2006) 626–631.
[13] A.L. Ohlsson, B.B. Johansson, Environment influences functional outcome of cerebral infarction in rats, Stroke 26 (1995) 644–649.
[14] M. Ploughman, S. Granter-Button, G. Chernenko, B.A. Tucker, K.M. Mearow, D. Corbett, Endurance exercise regimens induce differential effects on brain-derived neurotrophic factor, synapsin-I and insulin-like growth factor I after focal ischemia, Neuroscience 136 (2005) 991–1001.
[15] A. Risedal, B. Mattsson, P. Dahlqvist, C. Nordborg, T. Olsson, B.B. Johansson, Environmental influences on functional outcome after a cortical infarct in the rat, Brain Res. Bull. 58 (2002) 315–321.
[16] Y. Shono, C. Yokota, Y. Kuge, S. Kido, A. Harada, K. Kokame, H. Inoue, M. Hotta, K. Hirata, H. Saji, N. Tamaki, K. Minematsu, Gene expression associated with an enriched environment after transient focal ischemia, Brain Res. 1376 (2011) 60–65.
[17] H.K. Teng, K.K. Teng, R. Lee, S. Wright, S. Tevar, R.D. Almeida, P. Kermani, R. Torkin, Z.Y. Chen, F.S. Lee, R.T. Kraemer, A. Nykjaer, B.L. Hempstead, ProBDNF induces neuronal apoptosis via activation of a receptor complex of p75NTR and sortilin, J. Neurosci. 25 (2005) 5455–5463.
[18] K. Tureyen, N. Brooks, K. Bowen, J. Svaren, R. Vemuganti, Transcription factor early growth response-1 induction mediates inflammatory gene expression and brain damage following transient focal ischemia, J. Neurochem. 105 (2008) 1313–1324.
[19] L.R. Zhao, B. Mattsson, B.B. Johansson, Environmental influence on brain-derived neurotrophic factor messenger RNA expression after middle cerebral artery occlusion in spontaneously hypertensive rats, Neuroscience 97 (2000) 177–184.
[20] L.R. Zhao, A. Risedal, A. Wojcik, J. Hejzlar, B.B. Johansson, Z. Kokaia, Enriched environment influences brain-derived neurotrophic factor levels in rat forebrain after focal stroke, Neurosci. Lett. 305 (2001) 169–172.

ultrastructural and functional characterization. *J Thromb Haemost* 2010; **8**: 173–84.
13 Mangin P, Yap CL, Nonne C, Sturgeon SA, Goncalves I, Yuan Y, Schoenwaelder SM, Wright CE, Lanza F, Jackson SP. Thrombin overcomes the thrombosis defect associated with platelet GPVI/FcRgamma deficiency. *Blood* 2006; **107**: 4346–53.
14 Kalia N, Auger JM, Atkinson B, Watson SP. Critical role of FcR gamma-chain, LAT, PLCgamma2 and thrombin in arteriolar thrombus formation upon mild, laser-induced endothelial injury *in vivo*. *Microcirculation* 2008; **15**: 325–35.
15 Konstantinides S, Ware J, Marchese P, Mus-Jacobs F, Loskutoff DJ, Ruggeri ZM. Distinct antithrombotic consequences of platelet glycoprotein Ibalpha and VI deficiency in a mouse model of arterial thrombosis. *J Thromb Haemost* 2006; **4**: 2014–21.
16 Massberg S, Gawaz M, Gruner S, Schulte V, Konrad I, Zohlnhofer D, Heinzmann U, Nieswandt B. A crucial role of glycoprotein VI for platelet recruitment to the injured arterial wall *in vivo*. *J Exp Med* 2003; **197**: 41–9.
17 Eckly A, Hechler B, Freund M, Zerr M, Cazenave JP, Lanza F, Mangin PH, Gachet C. Mechanisms underlying FeCl(3) -induced arterial thrombosis. *J Thromb Haemost* 2011; **9**: 779–89.
18 Inoue O, Suzuki-Inoue K, McCarty OJ, Moroi M, Ruggeri ZM, Kunicki TJ, Ozaki Y, Watson SP. Laminin stimulates spreading of platelets through integrin alpha6beta1-dependent activation of GPVI. *Blood* 2006; **107**: 1405–12.
19 Brill A. A ride with ferric chloride. *J Thromb Haemost* 2011; **9**: 776–8.
20 Wong LC, Langille BL. Developmental remodeling of the internal elastic lamina of rabbit arteries: effect of blood flow. *Circ Res* 1996; **78**: 799–805.
21 Marsh LE, Lewis SD, Lehman ED, Gardell SJ, Motzel SL, Lynch JJ Jr. Assessment of thrombin inhibitor efficacy in a novel rabbit model of simultaneous arterial and venous thrombosis. *Thromb Haemost* 1998; **79**: 656–62.
22 Pinel C, Wice SM, Hiebert LM. Orally administered heparins prevent arterial thrombosis in a rat model. *Thromb Haemost* 2004; **91**: 919–26.
23 Wang X, Cheng Q, Xu L, Feuerstein GZ, Hsu MY, Smith PL, Seiffert DA, Schumacher WA, Ogletree ML, Gailani D. Effects of factor IX or factor XI deficiency on ferric chloride-induced carotid artery occlusion in mice. *J Thromb Haemost* 2005; **3**: 695–702.
24 Pozgajova M, Sachs UJ, Hein L, Nieswandt B. Reduced thrombus stability in mice lacking the alpha2A-adrenergic receptor. *Blood* 2006; **108**: 510–4.

von Willebrand factor-to-ADAMTS13 ratio increases with age in a Japanese population

K. KOKAME,* T. SAKATA,† Y. KOKUBO‡ and T. MIYATA*
**Department of Molecular Pathogenesis, †Laboratory of Clinical Chemistry* and *‡Department of Preventive Cardiology, National Cerebral and Cardiovascular Center, Suita, Osaka, Japan*

To cite this article: Kokame K, Sakata T, Kokubo Y, Miyata T. von Willebrand factor-to-ADAMTS13 ratio increases with age in a Japanese population. *J Thromb Haemost* 2011; **9**: 1426–8.

ADAMTS13, a plasma metalloprotease, regulates platelet aggregation through shear stress-dependent specific cleavage of von Willebrand factor (VWF) multimers. Severe deficiency of plasma ADAMTS13 activity results in accumulation of unusually high-molecular-weight VWF multimers in plasma, and can cause a systemic disease, thrombotic thrombocytopenic purpura (TTP) [1–3]. Previously, we developed a simple and quantitative assay for measuring ADAMTS13 activity using FRETS-VWF73, a fluorogenic peptide substrate [4]. In this study, we used the assay to measure plasma ADAMTS13 activity in 3616 individuals from the Japanese general population.

We used plasma samples from the previously published Suita Study [5–7], an epidemiological study consisting of randomly selected Japanese residents of the city of Suita, which is located in the second largest urban area in Japan. Participants between the ages of 30 and 79 years were randomly selected from the municipality population registry and stratified into groups by sex and age in 10-year increments in 1989. They underwent regular health check-ups between September 1989 and March 1994. Subjects have continued to visit the National Cerebral and Cardiovascular Center every 2 years for regular health check-ups. Our study protocol was approved by the ethical review committee, and only subjects who provided written informed consent for genetic analyses were included.

When the mean of all plasma ADAMTS13 activity values was set at 100%, the standard deviation (SD) was 27% (Fig. 1A). The fifth percentile, 25th percentile, median, 75th percentile and 95th percentile were 61%, 81%, 97%, 116% and 148%, respectively. The mean activity of men (93 ± 24%, mean ± SD, n = 1687) was significantly lower ($P < 0.0001$) than that of women (106 ± 27%, n = 1929), consistent with the previous report [4].

In both men and women, the plasma ADAMTS13 activity tended to decrease with age, especially after age 60 (Fig. 1B). A linear regression model also indicated the decrease with age (regression coefficient of −0.642 and 95% confidence intervals (CI) of −0.740 to −0.544 in men; −0.663 and −0.767 to −0.558 in women). We also measured plasma VWF antigen levels

Correspondence: Koichi Kokame, Department of Molecular Pathogenesis, National Cerebral and Cardiovascular Center, 5-7-1 Fujishirodai, Suita, Osaka 565-8565, Japan.
Tel.: +81 6 6833 5012; fax: +81 6 6835 1176.
E-mail: kame@ri.ncvc.go.jp

DOI: 10.1111/j.1538-7836.2011.04333.x

Received 30 March 2011, accepted 24 April 2011

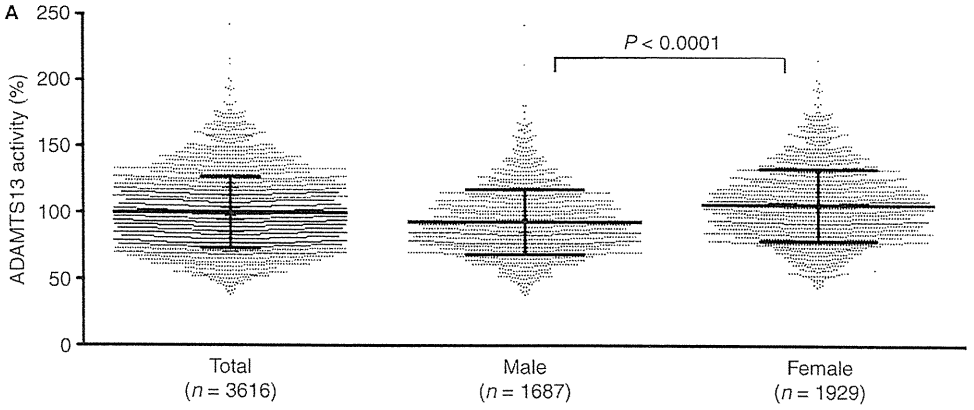

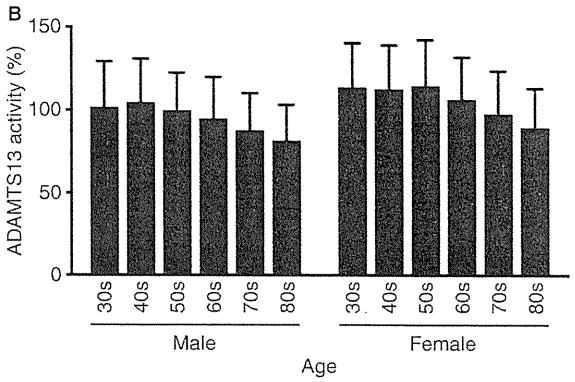

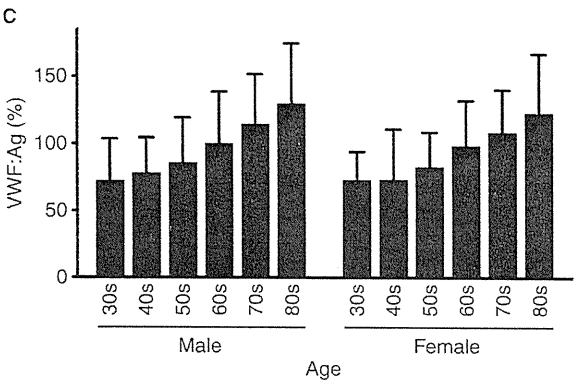

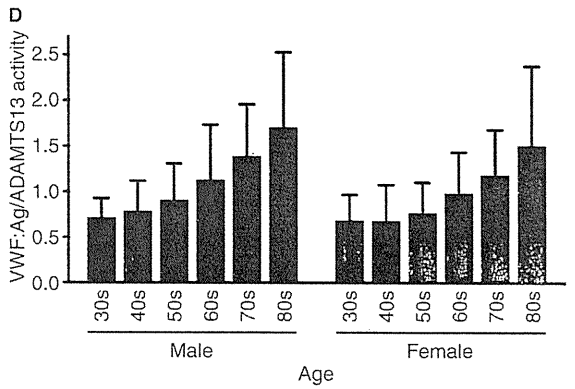

E

		Q1	Q2	Q3	Q4
Male $n = 1687$	ADAMTS13 activity (%)	38–76	76–90	90–109	109–242
	VWF:Ag (%) ± SE	107 ± 11	106 ± 11	108 ± 11	111 ± 11
		$P = 0.153$			
Female $n = 1929$	ADAMTS13 activity (%)	44–86	86–104	104–123	123–216
	VWF:Ag (%) ± SE	103 ± 9	99 ± 10	99 ± 10	101 ± 9
		$P = 0.670$			

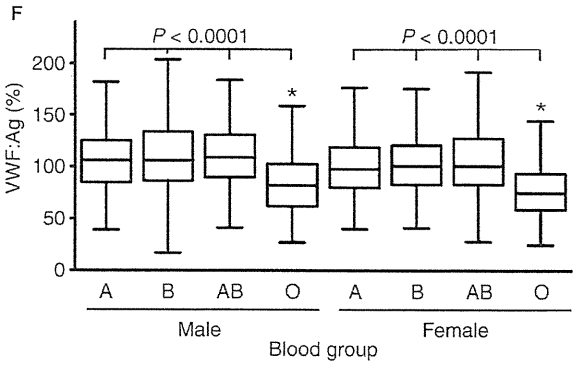

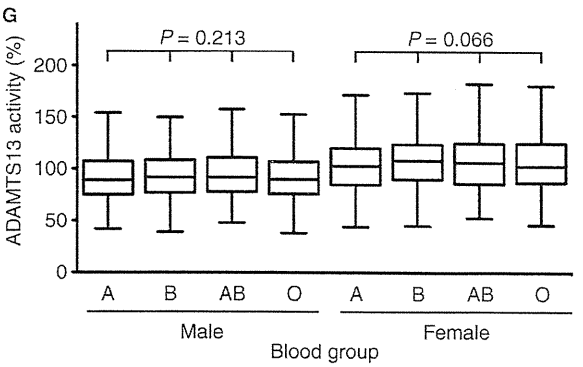

Fig. 1. Plasma ADAMTS13 activity in a Japanese general population. (A) Scatter dot plot of total, male and female plasma ADAMTS13 activity. The mean of all values was set at 100%. Lines indicate the means with SD. *P*, *t*-test. (B, C, D) Age-specific ADAMTS13 activity (B), VWF:Ag (C) and VWF:Ag-to-ADAMTS13 activity ratio (D). The mean of all VWF:Ag values was set at 100%. Error bars indicate SD. (E) Analysis of VWF:Ag by quartiles of plasma ADAMTS13 activity. *P*, ANCOVA. (F, G) Box-and-whisker plot of blood group-specific VWF:Ag (F) and ADAMTS13 activity (G). *P*, Kruskal–Wallis test. *Only blood group O had significantly different VWF:Ag from other blood groups.

(VWF:Ag) of all subjects using an immuno-turbidimetric assay, STA LIATEST VWF (Diagnostica Stago, Parsippany, NJ, USA). In both men and women, VWF:Ag increased with age (Fig. 1C), as reported previously [8]. The linear regression coefficient was 1.37 (95% CI, 1.21–1.52) in men and 1.30 (1.17–1.42) in women. Because of combined effects of the increase in VWF:Ag and the decrease in ADAMTS13 activity, the VWF:Ag-to-ADAMTS13 activity ratio was dramatically increased with age (Fig. 1D). This may partly explain the prothrombotic state of elderly men and women, because the imbalance between VWF and ADAMTS13 may be involved in thrombotic diseases such as acute myocardial infarction [9], advanced liver cirrhosis [10] and coronary artery disease [11]. As the FRETS-VWF73 assay itself was not affected by VWF concentration in plasma samples (0–160 $\mu g\ mL^{-1}$, data not shown), the reduced ADAMTS13 activity in the plasma of elderly subjects was not considered to be due to the assay-dependent artifactual phenomenon. In fact, when age-adjusted VWF:Ag was compared among quartiles of ADAMTS13 activity in the population using SPSS Statistics (IBM, Tokyo, Japan), no significant association between VWF:Ag and ADAMTS13 activity was observed in men (ANCOVA, $P = 0.153$) or in women ($P = 0.670$) (Fig. 1E).

ABO blood group has a significant influence on VWF:Ag; individuals with blood group O have lower VWF:Ag values than those of non-O groups [8]. We genotyped the ABO blood group by TaqMan assay (Applied Biosystems, Tokyo, Japan), which detects two polymorphisms, c.261Gdel and c.526C > G, on *ABO*. As expected, the subjects of blood group O exhibited a significantly lower VWF:Ag (men, 88 ± 43%; women, 80 ± 28%, mean ± SD) than those of the other blood groups (men A, 110 ± 35%; men B, 112 ± 36%; men AB, 115 ± 44%; women A, 103 ± 37%; women B, 105 ± 36%; women AB, 106 ± 31%) (Fig. 1F). In contrast, the plasma ADAMTS13 activity in men (A, 92 ± 24%; B, 94 ± 24%; AB, 96 ± 24%; O, 93 ± 25%) and women (A, 104 ± 26%; B, 109 ± 28; AB, 109 ± 28%; O, 106 ± 28) was not significantly associated with ABO blood group (Fig. 1G). This is consistent with the finding that ADAMTS13 antigen levels are not associated with ABO blood group in 387 male subjects [12]. The results are also consistent with the fact that VWF [13] but not ADAMTS13 [14] contains ABO blood group-related N-linked oligosaccharides.

In conclusion, this study demonstrated that, in the Japanese general population, the plasma ADAMTS13 activity is lower in men than in women, decreases with age, and is not significantly associated with ABO blood group. The VWF:Ag-to-ADAMTS13 activity ratio is increased with age in both men and women, and this increase may be involved in the prothrombotic state of elderly individuals.

Acknowledgements

This work was supported by grants-in-aid from the Ministry of Health, Labour, and Welfare of Japan; from the Ministry of Education, Culture, Sports, Science and Technology of Japan; and from the Program for Promotion of Fundamental Studies in Health Sciences of the National Institute of Biomedical Innovation (NIBIO) of Japan.

Disclosure of conflict of interests

The authors state that they have no conflict of interest.

References

1 Sadler JE. von Willebrand factor, ADAMTS13, and thrombotic thrombocytopenic purpura. *Blood* 2008; **112**: 11–8.
2 Moake J. Thrombotic microangiopathies: multimers, metalloprotease, and beyond. *Clin Transl Sci* 2009; **2**: 366–73.
3 Tsai HM. Pathophysiology of thrombotic thrombocytopenic purpura. *Int J Hematol* 2010; **91**: 1–19.
4 Kokame K, Nobe Y, Kokubo Y, Okayama A, Miyata T. FRETS-VWF73, a first fluorogenic substrate for ADAMTS13 assay. *Br J Haematol* 2005; **129**: 93–100.
5 Sakata T, Mannami T, Baba S, Kokubo Y, Kario K, Okamoto A, Kumeda K, Ohkura N, Katayama Y, Miyata T, Tomoike H, Kato H. Potential of free-form TFPI and PAI-1 to be useful markers of early atherosclerosis in a Japanese general population (the Suita Study): association with the intimal-medial thickness of carotid arteries. *Atherosclerosis* 2004; **176**: 355–60.
6 Kimura R, Kokubo Y, Miyashita K, Otsubo R, Nagatsuka K, Otsuki T, Sakata T, Nagura J, Okayama A, Minematsu K, Naritomi H, Honda S, Sato K, Tomoike H, Miyata T. Polymorphisms in vitamin K-dependent γ-carboxylation-related genes influence interindividual variability in plasma protein C and protein S activities in the general population. *Int J Hematol* 2006; **84**: 387–97.
7 Kokubo Y, Kamide K, Okamura T, Watanabe M, Higashiyama A, Kawanishi K, Okayama A, Kawano Y. Impact of high-normal blood pressure on the risk of cardiovascular disease in a Japanese urban cohort: the Suita study. *Hypertension* 2008; **52**: 652–9.
8 Gill JC, Endres-Brooks J, Bauer PJ, Marks WJ Jr, Montgomery RR. The effect of ABO blood group on the diagnosis of von Willebrand disease. *Blood* 1987; **69**: 1691–5.
9 Matsukawa M, Kaikita K, Soejima K, Fuchigami S, Nakamura Y, Honda T, Tsujita K, Nagayoshi Y, Kojima S, Shimomura H, Sugiyama S, Fujimoto K, Yoshimura M, Nakagaki T, Ogawa H. Serial changes in von Willebrand factor-cleaving protease (ADAMTS13) and prognosis after acute myocardial infarction. *Am J Cardiol* 2007; **100**: 758–63.
10 Uemura M, Fujimura Y, Matsumoto M, Ishizashi H, Kato S, Matsuyama T, Isonishi A, Ishikawa M, Yagita M, Morioka C, Yoshiji H, Tsujimoto T, Kurumatani N, Fukui H. Comprehensive analysis of ADAMTS13 in patients with liver cirrhosis. *Thromb Haemost* 2008; **99**: 1019–29.
11 Miura M, Kaikita K, Matsukawa M, Soejima K, Fuchigami S, Miyazaki Y, Ono T, Uemura T, Tsujita K, Hokimoto S, Sumida H, Sugiyama S, Matsui K, Yamabe H, Ogawa H. Prognostic value of plasma von Willebrand factor-cleaving protease (ADAMTS13) antigen levels in patients with coronary artery disease. *Thromb Haemost* 2010; **103**: 623–9.
12 Chion CKNK, Doggen CJM, Crawley JTB, Lane DA, Rosendaal FR. ADAMTS13 and von Willebrand factor and the risk of myocardial infarction in men. *Blood* 2007; **109**: 1998–2000.
13 Matsui T, Titani K, Mizuochi T. Structures of the asparagine-linked oligosaccharide chains of human von Willebrand factor: occurrence of blood group A, B, and H(O) structures. *J Biol Chem* 1992; **267**: 8723–31.
14 Hiura H, Matsui T, Matsumoto M, Hori Y, Isonishi A, Kato S, Iwamoto T, Mori T, Fujimura Y. Proteolytic fragmentation and sugar chains of plasma ADAMTS13 purified by a conformation-dependent monoclonal antibody. *J Biochem* 2010; **148**: 403–11.

THE JOURNAL OF BIOLOGICAL CHEMISTRY VOL. 286, NO. 29, pp. 26158–26165, July 22, 2011

NDRG4 Protein-deficient Mice Exhibit Spatial Learning Deficits and Vulnerabilities to Cerebral Ischemia*[S]

Received for publication, May 2, 2011, and in revised form, May 29, 2011 Published, JBC Papers in Press, June 2, 2011, DOI 10.1074/jbc.M111.256446

Hitomi Yamamoto[‡], Koichi Kokame[‡1], Tomohiko Okuda[‡], Yukako Nakajo[§], Hiroji Yanamoto[§2], and Toshiyuki Miyata[‡]

From the [‡]Department of Molecular Pathogenesis and [§]Laboratory of Neurology and Neurosurgery, National Cerebral and Cardiovascular Center, Suita, Osaka 565-8565, Japan

The N-myc downstream-regulated gene (NDRG) family consists of four related proteins, NDRG1-NDRG4, in mammals. We previously generated NDRG1-deficient mice that were unable to maintain myelin sheaths in peripheral nerves. This condition was consistent with human hereditary motor and sensory neuropathy, Charcot-Marie-Tooth disease type 4D, caused by a nonsense mutation of NDRG1. In contrast, the effects of genetic defects of the other NDRG members remain unknown. In this study, we focused on NDRG4, which is specifically expressed in the brain and heart. *In situ* mRNA hybridization on the brain revealed that NDRG4 was expressed in neurons of various areas. We generated NDRG4-deficient mice that were born normally with the expected Mendelian frequency. Immunochemical analysis demonstrated that the cortex of the NDRG4-deficient mice contained decreased levels of brain-derived neurotrophic factor (BDNF) and normal levels of glial cell line-derived neurotrophic factor, NGF, neurotrophin-3, and TGF-β1. Consistent with BDNF reduction, NDRG4-deficient mice had impaired spatial learning and memory but normal motor function in the Morris water maze test. When temporary focal ischemia of the brain was induced, the sizes of the infarct lesions were larger, and the neurological deficits were more severe in NDRG4-deficient mice compared with the control mice. These findings indicate that NDRG4 contributes to the maintenance of intracerebral BDNF levels within the normal range, which is necessary for the preservation of spatial learning and the resistance to neuronal cell death caused by ischemic stress.

N-myc downstream-regulated gene (NDRG)[3] family members NDRG1-NDRG4 are intracellular proteins, consist of 340–394 amino acid residues, and share 53–65% sequence identity with each other. Furthermore, accumulating evidence implicates their roles in development, cancer metastasis, and the immune system (1–5).

We originally identified RTP (NDRG1) as a homocysteine-responsive gene in human umbilical vein endothelial cells (6), which is also called DRG1, Cap43, Rit42, Ndr1, and PROXY-1. NDRG1 expression is induced by a number of conditions, such as DNA damage, hypoxia, and intracellular calcium ion elevation (4). Overexpression of NDRG1 suppresses the metastatic potency of some types of cancer cells (4) and enhances the degranulation of mast cells in response to various stimuli (7). A nonsense mutation of *NDRG1* causes hereditary motor and sensory neuropathy, Charcot-Marie-Tooth disease type 4D, which presents as distal muscle wasting and atrophy, foot and hand deformities, tendon areflexia, sensory loss, and deafness in afflicted individuals (8). We previously generated NDRG1-deficient mice and revealed the essential role of NDRG1 in the cytoplasm of Schwann cells for the maintenance of myelin sheaths in peripheral nerves (9). A frame shift deletion of *Ndrg1* in Greyhounds also causes polyneuropathy (10).

Similar to NDRG1, the expression of NDRG2 is induced by stress conditions such as hypoxia (1). NDRG2 expression is up-regulated in cortical pyramidal neurons, senile plaques, and the cellular process of dystrophic neurons in the Alzheimer's brain, whereas expression is decreased in the rat frontal cortex after antidepressant treatment and electroconvulsive therapy (11). NDRG2 also plays a role in aldosterone-mediated epithelial sodium channel function (12), dendritic cell differentiation (13), and insulin action (14). NDRG3, on the other hand, may play a role in spermatogenesis because it is found in the outer layers of the seminiferous epithelium (3). Overexpression of NDRG3 contributes to the angiogenesis of tumors via up-regulation of chemokines (3).

In contrast to other NDRG members, NDRG4 expression is detected specifically in the brain and heart (15). In the embryonic mouse heart, NDRG4 expression is down-regulated under severe ventricular hypoplasia caused by Tbx2 misexpression, implying that NDRG4 is involved in cell growth and proliferation (16). However, information on the physiological function of NDRG4 is lacking. In the mouse brain, NDRG4 is identified in the neuronal cytoplasm of the cerebrum and cerebellum (17). Down-regulation of NDRG4 in PC12 cells results in extending shorter neurites in response to NGF (18). Considering that NDRG4 expression is induced by treatment with homocysteine in rat aortic smooth muscle cells (19), we speculated that

* This work was supported by grants-in-aid from the Ministry of Health, Labor, and Welfare of Japan; from the Ministry of Education, Culture, Sports, Science and Technology of Japan; and from the Program for Promotion of Fundamental Studies in Health Sciences of the National Institute of Biomedical Innovation (NIBIO) of Japan.

[S] The on-line version of this article (available at http://www.jbc.org) contains supplemental Fig. S1.

[1] To whom correspondence may be addressed: 5-7-1 Fujishirodai, Suita, Osaka 565-8565, Japan. Fax: 81-6-6835-1176; E-mail: kame@ri.ncvc.go.jp.

[2] To whom correspondence may be addressed: 5-7-1 Fujishirodai, Suita, Osaka 565-8565, Japan. Fax: 81-6-6835-6894; E-mail: hyanamot@res.ncvc.go.jp.

[3] The abbreviations used are: NDRG, N-myc downstream-regulated gene; BDNF, brain-derived neurotrophic factor; GDNF, glial cell line-derived neurotrophic factor; NT-3, neurotrophin-3; GFAP, glial fibrillary acidic protein; MCAO, middle cerebral artery occlusion; rCBF, regional cerebral blood flow.

NDRG4 is stress-related and has a cell-protective role in neurological disorders and cerebrovascular disease. This was supported by our finding that NDRG4 mRNA expression is decreased in the brain of patients with Alzheimer's disease (15).

Neurotrophins such as brain-derived neurotrophic factor (BDNF), glial cell line-derived neurotrophic factor (GDNF), NGF, neurotrophin-3 (NT-3), and TGF-β1 are essential for the survival and homeostatic maintenance of central neurons (20). BDNF, especially, is a potent modulator of synaptic connectivity in the central nervous system, influencing synaptic structure and function. The reduced levels of BDNF in the entorhinal cortex or forebrain are associated with poor memory (21, 22). BDNF also has neuroprotective action in models of ischemia. Increased BDNF levels in the brain for an appropriate period prior to the ischemic insult increases the resistance of the brain against lethal stresses caused by severe ischemia (23, 24). In contrast, a deficiency in endogenous BDNF renders the brain more susceptible to ischemic injury (25) and more suppressive to infarct tolerance by the preconditioning of spreading depression (26).

In this study, we generated NDRG4-deficient mice to reveal the roles of NDRG4 in the brain. As a result, we found that under the condition of NDRG4 deficiency, mice showed impaired phenotypes in spatial learning and neuroprotection with decreased levels of BDNF.

EXPERIMENTAL PROCEDURES

Antibodies—Anti-NDRG1 rabbit antiserum was raised against recombinant glutathione S-transferase-fusion protein of human NDRG1 (27). Anti-NDRG2, anti-NDRG3, and anti-NDRG4 rabbit antisera were raised against the synthetic peptides Q^{351}SSESGTLPSGPPGH^{365} for mouse NDRG2 (17), F^{343}SRSVTSNQSDGTQE^{357} for mouse NDRG3 (17), and C-N^{214}RPGTVPNAKTLR^{226}-$CONH_2$ for mouse NDRG4, respectively, which were conjugated with keyhole limpet hemocyanin. Polyclonal antibodies in the antisera were purified by antigen-immobilized affinity column chromatography. Anti-NeuN and anti-glial fibrillary acidic protein (GFAP) were purchased from Millipore and Dako, respectively.

Construction of the Targeting Vector—We previously isolated and characterized genomic clones carrying *NDRG4* (15). The NDRG4-B and NDRG4-B^{var} isoforms are the alternative splicing products, whereas the NDRG4-H isoform is produced by the alternative promoter usage. The initiating Met codons for NDRG4-B/B^{var} and NDRG4-H exist in exons 5 and 3, respectively. Exon 6 is common to all isoforms. The loxP-flanked pST-neoB cassette (28) was inserted within exon 6. The ~11-kb sequence was inserted into the diphtheria toxin A fragment cassette vector (29), and the DNA was linearized by SalI digestion for electroporation.

Generation of NDRG4-deficient Mice—R1 mouse embryonic stem cells (30) were electroporated with the targeting vector and selected in medium containing G418. Targeted clones were identified by Southern blotting using the Gene Images Random-prime system (GE Healthcare) with 5′- and 3′-external probes. These cells were injected into blastocysts to obtain chimeras, which were crossed with wild-type C57BL/6 mice (Japan SLC) for germ line transmission of the disrupted *Ndrg4* allele. The genotypes of the offspring were examined by PCR analysis of DNA isolated from ear biopsy using three primers; P1 (CATCTCTCCAAGAGCCAGAGTGT), P2 (AAGATGCAGCCACACTTACGATT), and P3 (AACAGTAACAGCTTCCCACATC). Heterozygous mice with the disrupted *Ndrg4* allele were backcrossed with wild-type C57BL/6 mice. The mouse experiments were approved by the Animal Care and Use Committee of the National Cerebral and Cardiovascular Center in Japan, and were performed in accordance with the institutional and national guidelines and regulations.

Western Blotting Analysis—Protein expression was analyzed by Western blotting as described previously (31). Briefly, organs perfused with PBS (10 mM sodium phosphate, 150 mM NaCl (pH 7.4)) were homogenized in SDS sample buffer (10 mM Tris-HCl, 2% SDS, 50 mM DTT, 2 mM EDTA, 0.02% bromphenol blue, 6% glycerol (pH 6.8)), boiled for 7 min, and subjected to SDS-PAGE. Proteins in the gels were transferred to an immunoblot PVDF membrane (Bio-Rad). Following a blocking step with 5% skim milk, the membrane was incubated with anti-NDRG4, anti-NDRG1, anti-NDRG2, or anti-NDRG3 and probed with HRP-labeled goat anti-rabbit IgG (Kirkegaard and Perry Laboratories). The membrane was developed using Immobilon Western chemiluminescent HRP substrate (Millipore), and chemiluminescence was detected by a LAS-3000 image analyzer (GE Healthcare).

In Situ mRNA Hybridization—Digoxigenin-labeled riboprobes were prepared for nucleotide positions 1269–1777 (NDRG4-a) and 1811–2343 (NDRG4-b) of mouse NDRG4 (NM_145602). The paraffin-embedded brain sections (6 μm thick) were dewaxed, rehydrated, and treated with proteinase K (8 μg/ml) for 30 min at 37 °C. The sections were acetylated by 0.25% acetic anhydride and hybridized with the riboprobes (300 ng/ml) for 16 h at 60 °C. Following treatment with RNase A (50 μg/ml) for 30 min at 37 °C and 0.5% blocking reagent (Roche), the sections were incubated with anti-DIG alkaline phosphate conjugate (Roche). Colorimetric reactions were performed with nitro blue tetrazolium chloride/5-bromo-4-chloro-3-indolyl phosphate solution (Sigma), and then the sections were counterstained with Kernechtrot stain solution (Mutoh). Because NDRG4-a and NDRG4-b riboprobes exhibited quite similar performance, only the data from NDRG4-a riboprobes are shown.

Immunohistochemistry—Serial sections for *in situ* mRNA hybridization were deparaffinized, rehydrated, and boiled by microwave irradiation in 10 mM citrate buffer (pH 6.0). After incubation with 0.3% hydrogen peroxide, the sections were blocked, incubated with anti-NeuN, and stained using Histofine MOUSESTAIN Kit (Nichirei) and diaminobenzidine according to the manufacturer's instructions. Alternate sections were blocked with Protein Block Serum-Free (Dako) and the Avidin/Biotin blocking kit (Vector Laboratories), and then incubated with anti-GFAP. Following incubation with biotin-conjugated goat anti-rabbit Ig (Dako), the sections were treated with HRP-conjugated streptavidin (Nichirei) and stained with diaminobenzidine. The sections were counterstained with Mayer's hematoxylin (Mutoh).

Measurement of Neurotrophin Levels—Protein levels of BDNF, GDNF, NGF, NT-3, and TGF-β1 were measured as

described (32). The PBS-perfused cerebral cortex described above was excised from each mouse (7–18 weeks old) and homogenized. The protein levels were measured using a two-site sandwich ELISA, Emax Immunoassay System (Promega). The protein concentration in each sample was measured using a BCA protein assay kit (Thermo Scientific).

Morris Water Maze (MWM) Test—We conducted the MWM test (33) using modifications as described previously (32). In a 64 × 91 cm-sized pool of opaque water (from a non-toxic agent), a 10 × 10 cm-square-shaped platform was hidden at a fixed position 2 cm under the surface of the water. The temperature of the water was kept at 24–25 °C during the procedure. Each mouse (6–8 weeks old) performed four trials per day, over five consecutive days, without any prior or subsequent training. We defined a successful escape, *i.e.* standing on the platform, as a stop for more than 1 s with all limbs on the platform. The cut-off time in a trial was set at 300 s. Mice that failed to reach the platform in 300 s were removed from the water, and the time needed to escape to the platform (escape latency) became 300 s. In each trial, the escape latency, the total path length needed to navigate to the platform, and the maximum swimming speed were analyzed using a video-tracking system, Smart (Panlab).

Middle Cerebral Artery Occlusion (MCAO) Model—Temporary focal ischemia was induced using the three-vessel occlusion technique as described previously (34). Briefly, under halothane-inhalation anesthesia, the left middle cerebral artery of each mouse (8–19 weeks old) was cauterized at the lateral border of the olfactory tract, and bilateral common carotid arteries were clip-occluded for 15 min followed by reperfusion. After opening the skull and subsequent cauterization of the MCA, the wound for the surgical MCA obstruction was closed within 3 min to avoid hypothermic neuroprotection against reperfusion injury (35). The rectal temperature was regulated so that it stayed within the physiological range (36.5–37.5 °C) using a temperature controller (NS-TC10, Neuroscience) during the operation. The heart rate and mean blood pressure were monitored via the tail artery using indirect blood pressure meter BP-98AW (Softron).

Regional Cerebral Blood Flow (rCBF) in the Penumbra-like Peripheral Area—The rCBF was monitored using the laser-Doppler blood flowmetry meter TBF-LN1 (Unique Medical) (34). The measurement area was set in the penumbra-like peripheral area of the ischemic region at 2 mm caudal and 1 mm dorsal to the crossover point of the left middle cerebral artery and the lateral surface of the olfactory tract. The rCBF was measured just before (control), during, and after MCAO.

Cerebral Function—Twenty-four hours or 7 days after MCAO, neurological deficits were examined according to a published scoring scale, with some modifications (35). Balance in the body trunk while being lifted by the tail was graded according to the following criteria: 0, no deficit (no twisting of the body); 1, mild deficit (asymmetric twisting tendency of the body); and 2, severe deficit (repeated asymmetric twisting of the body). Motor function of the extremities while being lifted by the tail was graded as follows: 0, no deficit (symmetrical movement of the forelimbs); 1, mild deficit (intermittent asymmetrical flexion of the forelimbs); and 2, severe deficit (continuous asymmetrical flexion of the forelimbs). The neurological deficit score (from 0 to 4) comprises the sum of the grades of the balance in body trunk and motor function of extremities.

Measurement of Infarcted Volume—Mice were perfused transcardially with heparinized PBS at 24 h or 7 days after MCAO to wash out any blood components from the brain tissue, which visualizes intraluminal blood coagulation or thrombosis formation, if any. The brain was removed and cut from the frontal tip into 1-mm-thick slices. Viable tissue was stained red with 2% 2,3,5-triphenyltetrazolium chloride followed by fixation with 4% paraformaldehyde in PBS. The infarct and total hemispheric areas of each slice were measured by tracing the borders in a computer-assisted image-analysis system, WinROOF (Mitani). To assess the total infarct volume after MCAO, an edema index was calculated by dividing the total volume of the hemisphere ipsilateral to the MCAO by the volume of the contralateral hemisphere. The infarcted volume was adjusted by dividing the volume by the edema index. The value of edema index at 7 days after MCAO could be considered 1.00, as found in our previous study (35).

Statistical Analysis—Data are presented as the means ± S.D. We used unpaired Student's *t* tests for comparisons within each parameter. Probability values of < 0.05 were considered statistically significant.

RESULTS

Localization of NDRG4 in Mouse Brain—We performed *in situ* mRNA hybridization to investigate the cellular localization of NDRG4 in the adult mouse brain. NDRG4 mRNA was widely distributed in various parts of brain (Fig. 1, *A* and *B*), including the olfactory bulb, olfactory tuberculum, cerebral cortex, striatum, hippocampus, dentate gyrus, thalamus, hypothalamus, mesencephalon, cerebellum, pons, and medulla oblongata (supplemental Fig. S1). To identify the cell types that were positive for the NDRG4 riboprobe, we analyzed serial sections by *in situ* mRNA hybridization for NDRG4 (Fig. 1, *C* and *D*) in combination with immunostaining for NeuN, a marker of neurons (*E* and *F*) or GFAP, a marker of astrocytes (*G* and *H*). NDRG4 expression was mainly observed in NeuN-positive cells but not in GFAP-positive cells, indicating that NDRG4 was specifically expressed in neurons. This was consistent with our previous finding that NDRG4 protein was expressed in neurons of the cerebral cortex and Purkinje cells of the cerebellum (17).

Generation of NDRG4-deficient Mice—To elucidate the effects of NDRG4 deficiency in neuronal cells, we generated NDRG4 knockout mice using gene targeting strategies (Fig. 2*A*). The *Ndrg4* gene covers all NDRG4 protein isoforms, NDRG4-B, NDRG4-B^{var}, and NDRG4-H (15). The genomic DNA fragment encompassing exon 6, which is the most upstream common coding region of NDRG4 isoforms, was used to construct the targeting vector. The genotype was confirmed by genomic PCR analysis (Fig. 2*B*). The F1 mice with one *Ndrg4*-disrupted allele (*Ndrg4*$^{+/-}$) were backcrossed with wild-type C57BL/6 mice (*Ndrg4*$^{+/+}$). *Ndrg4*$^{+/-}$ mice were then crossed to generate the NDRG4-deficient mice (*Ndrg4*$^{-/-}$). *Ndrg4*$^{-/-}$ mice were born normally with the expected Mendelian distribution. The numbers of *Ndrg4*$^{+/+}$, *Ndrg4*$^{+/-}$, and *Ndrg4*$^{-/-}$ live births were 56, 115, and 51, respectively (p =

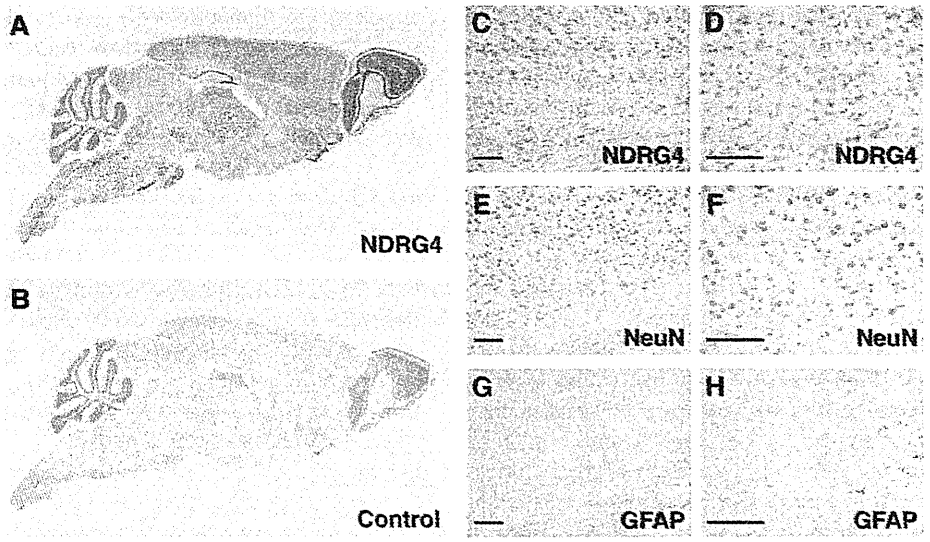

FIGURE 1. **Localization of NDRG4 in the mouse brain.** Sagittal sections were prepared from 8-week-old wild-type mice and subjected to *in situ* mRNA hybridization of NDRG4 (*A* and *B*). Digoxigenin-labeled antisense riboprobes for NDRG4 (*A*) but not sense riboprobes (*B*, negative control) produced positive signals (*blue*). The nuclei were counterstained in *red*. *C–H*, serial coronal sections of wild-type mouse brain were subjected to *in situ* mRNA hybridization of NDRG4 (*C* and *D*, *blue* signals) and immunostaining of NeuN (*E* and *F*, *brown* signals) or GFAP (*G* and *H*, *brown* signals). The nuclei were counterstained in *red* (*C* and *D*) and *blue* (*E–H*). *D*, *F*, and *H* are higher-magnification images of *C*, *E*, and *G*, respectively. *Scale bars* = 100 μm.

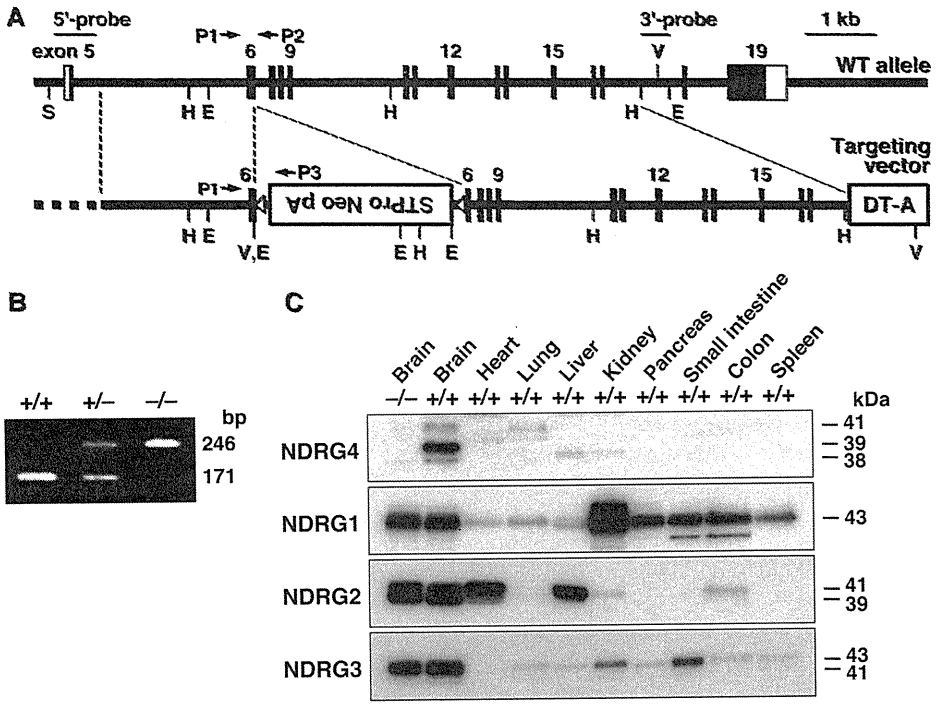

FIGURE 2. **Generation of NDRG4-deficient mice and expression pattern of NDRG family proteins in mouse organs.** *A*, targeting strategy for the *Ndrg4* gene knockout. *Solid boxes* represent open reading frames of *Ndrg4*. The loxP-flanked (*open triangles*) pSTneoB cassette with a polyadenylation signal (*STPro Neo pA*) was inserted into exon 6, and the diphtheria toxin A fragment cassette (*DT-A*) was included at the 3′ end of the vector. The 5′- and 3′-external probes used for Southern blotting selection of ES clones are shown by *bars*. The PCR primers (*P1*, *P2*, and *P3*) for genotyping are shown by *arrows*. *S*, SalI; *H*, HindIII; *E*, EcoRI; *V*, EcoRV. *B*, genotyping of wild-type (*Ndrg4*$^{+/+}$), heterozygous NDRG4-deficient (*Ndrg4*$^{+/-}$), and homozygous NDRG4-deficient (*Ndrg4*$^{-/-}$) mice. PCR amplification of the *Ndrg4*$^{+/+}$ and *Ndrg4*$^{-/-}$ alleles resulted in products of 171 and 246 bp, respectively. *C*, expression patterns of NDRG family proteins in mouse organs. Equal protein amount of organ homogenates from 17-week-old *Ndrg4*$^{-/-}$ and *Ndrg4*$^{+/+}$ mice were subjected to Western blotting analysis using each antibody. Anti-NDRG4 detected NDRG4-B (38 kDa), NDRG4-B^{var} (39 kDa), and NDRG4-H (41 kDa) in the *Ndrg4*$^{+/+}$ brain but not in the *Ndrg4*$^{-/-}$ brain. The expression of NDRG1, NDRG2, and NDRG3 was not affected by the lack of NDRG4 in the brain.

0.77, chi-square test). Both male and female *Ndrg4*$^{-/-}$ mice were fertile.

NDRGs Expression in Mouse Organs—To examine the expression patterns of NDRG family proteins in *Ndrg4*$^{+/+}$ and *Ndrg4*$^{-/-}$ mice, we performed a Western blotting analysis of their organs as adults. NDRG4 was specifically expressed in the brain, and little or no signal was detected in other tissues (Fig. 2*C*). The three isoforms, NDRG4-B (38 kDa), NDRG4-B^{var} (39

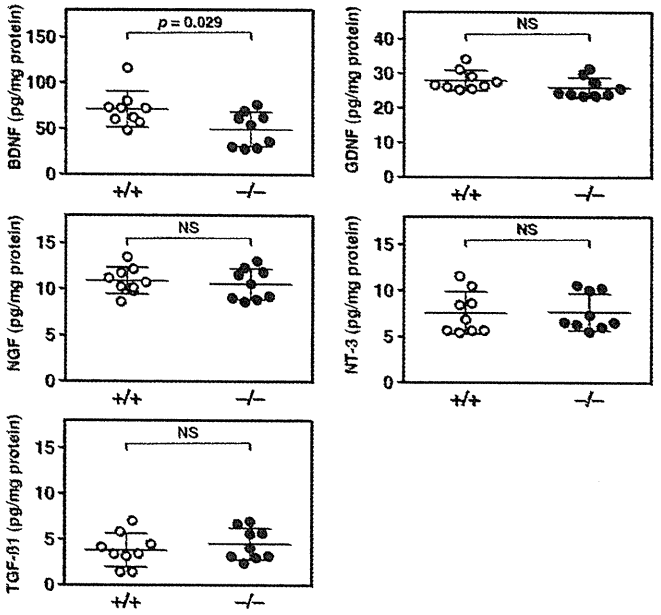

FIGURE 3. **Neurotrophins in the mouse cortex.** The protein levels of BDNF, GDNF, NGF, NT-3, and TGF-β1 in the cortex isolated from the *Ndrg4*$^{+/+}$ and *Ndrg4*$^{-/-}$ mice were measured by ELISA. Data are expressed as the mean ± S.D. ($n = 9$). *NS*, $p > 0.05$.

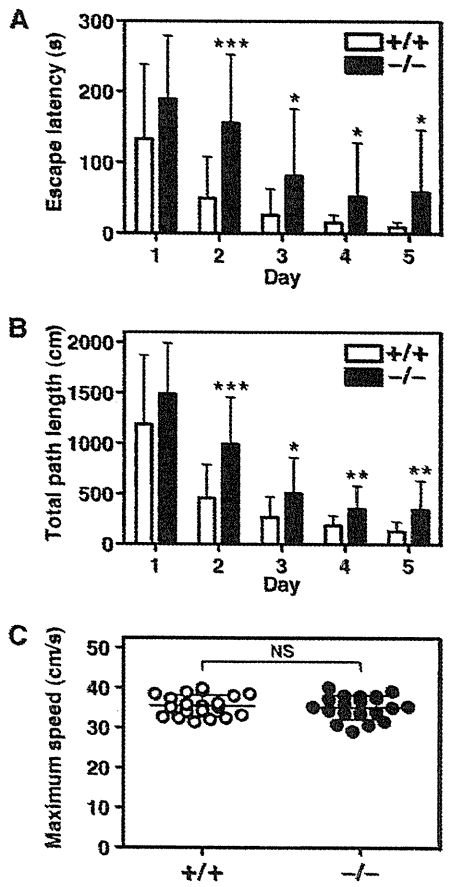

FIGURE 4. **MWM test.** Spatial learning and memory function of the *Ndrg4*$^{+/+}$ and *Ndrg4*$^{-/-}$ mice were tested in the MWM task. The escape latency (*A*), total path length (*B*), and maximum swimming speed (*C*) to the hidden platform on trials over five consecutive days are shown. The *Ndrg4*$^{-/-}$ mice exhibited inferior performance in escape latency and total path length in the MWM task as compared with *Ndrg4*$^{+/+}$ mice. However, the maximum swimming speed was equivalent between groups. Data are mean with error bars of S.D. ($n = 20$ in each experimental group). *, $p < 0.05$; **, $p < 0.01$; ***, $p < 0.001$; *NS*, $p > 0.05$.

kDa), and NDRG4-H (41 kDa), were detectable in the brain of *Ndrg4*$^{+/+}$ mice, whereas they were absent in the *Ndrg4*$^{-/-}$ brain. As described previously (15), NDRG1 was ubiquitously expressed in all tested organs. NDRG2 was mainly expressed in the brain, heart, and liver, with weaker expression in the kidney and colon. NDRG3 was observed in the brain, kidney, and small intestine. The expression levels of NDRG1, NDRG2, and NDRG3 in the brain were not affected by a lack of NDRG4, suggesting that there were no compensatory up-regulation mechanisms of gene expression.

Neurotrophin Levels—To investigate whether NDRG4 deficiency impacts brain function, we measured the protein levels of major neurotrophins in the brain (Fig. 3). The quantification of BDNF in the cortex homogenates revealed a significant decrease of BDNF in *Ndrg4*$^{-/-}$ (49.4 ± 18.8 pg/mg protein, $n = 9$) compared with *Ndrg4*$^{+/+}$ (71.1 ± 19.5 pg/mg protein, $n = 9$) mice. In contrast, the levels of GDNF, NGF, NT-3, and TGF-β1 in the cortex were not significantly different between the *Ndrg4*$^{+/+}$ and *Ndrg4*$^{-/-}$ mice (GDNF, 28.0 ± 3.0 *versus* 26.0 ± 3.0 pg/mg protein; NGF, 10.9 ± 1.4 *versus* 10.6 ± 1.7 pg/mg protein; NT-3, 7.6 ± 2.3 *versus* 7.7 ± 2.0 pg/mg protein; TGF-β1, 3.8 ± 1.8 *versus* 4.5 ± 1.7 pg/mg protein; $n = 9$). Therefore, we expected that abnormal regulation of BDNF protein levels may be involved in the development of the phenotypes of *Ndrg4*$^{-/-}$ mice.

Spatial Learning Ability—To confirm whether the lack of NDRG4 affects the ability of spatial learning and memory, we analyzed the performance of the mice in the MWM task. We found that escape latency to the hidden platform was significantly longer after the first trial for *Ndrg4*$^{-/-}$ mice compared with *Ndrg4*$^{+/+}$ mice (Fig. 4*A*). The total path length needed to navigate to the platform was also significantly longer in *Ndrg4*$^{-/-}$ than in *Ndrg4*$^{+/+}$ mice after the first trial (Fig. 4*B*). In contrast, there were no significant differences in the maximum swimming speed between *Ndrg4*$^{+/+}$ (35.5 ± 2.7 cm/s) and *Ndrg4*$^{-/-}$ (35.2 ± 3.0 cm/s) mice, indicating that *Ndrg4*$^{-/-}$ mice have normal sensorimotor function (Fig. 4C). These results indicated that poor performance of *Ndrg4*$^{-/-}$ mice in the MWM test was caused by the attenuation of spatial learning ability accompanied with BDNF reduction.

Neuronal Damage after Focal Ischemia—To elucidate whether NDRG4 is involved in the neuroprotective actions of BDNF, we explored the effect of NDRG4 deficiency on the development of neuronal damage after MCAO. We first performed transcardiac perfusion of PBS 24 h or 7 days after ischemia and confirmed that there was no thrombus formation except for the coagulated point in the proximal part of the middle cerebral artery in both *Ndrg4*$^{+/+}$ and *Ndrg4*$^{-/-}$ mice by visual inspection. A 2,3,5-triphenyltetrazolium chloride staining assay for viable cells at 24 h after a 15 min of MCAO demonstrated larger infarct lesion sizes in *Ndrg4*$^{-/-}$ mice compared with in *Ndrg4*$^{+/+}$ mice (Fig. 5, *A* and *B*). There were no differences in the edema index between the groups (1.07 ± 0.04 in *Ndrg4*$^{+/+}$ and 1.06 ± 0.03 in *Ndrg4*$^{-/-}$, $n = 10$). Corrobo-

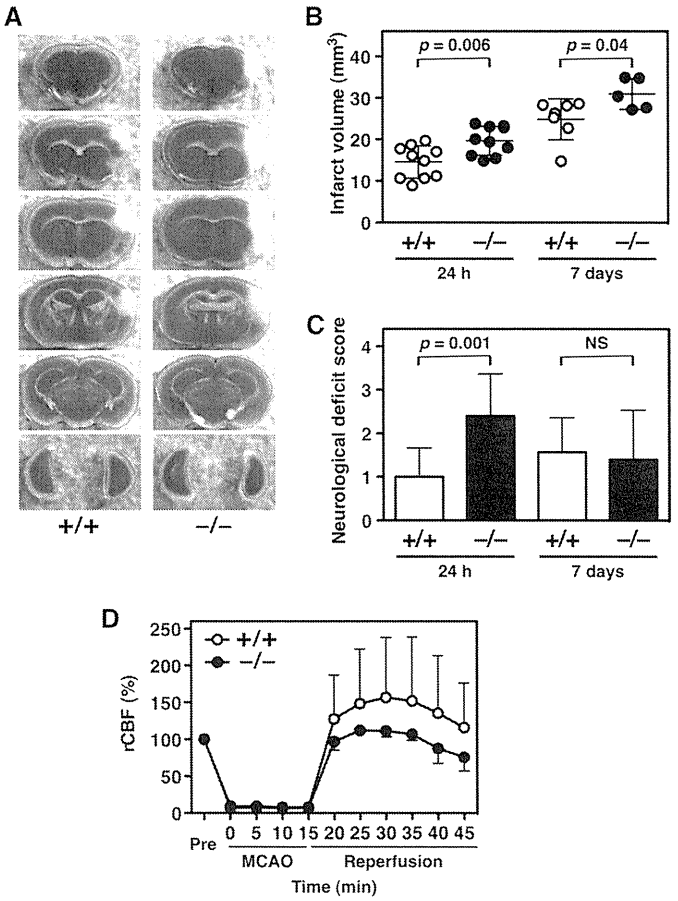

FIGURE 5. **Induction of temporary focal ischemia.** *A*, representative images of six corresponding coronal sections from *Ndrg4*$^{+/+}$ and *Ndrg4*$^{-/-}$ mouse brains at 24 h after MCAO. The 1-mm-thick slices were stained with 2,3,5-triphenyltetrazolium chloride. The sizes of infarcted region (*white area*) were larger in the brain slices of *Ndrg4*$^{-/-}$ mice compared with *Ndrg4*$^{+/+}$ mice. *B*, quantification of infarct volumes (mm^3) at 24 h and 7 days after MCAO. *Ndrg4*$^{-/-}$ mice (●) had larger infarct volumes than *Ndrg4*$^{+/+}$ mice (○). Data are mean ± S.D. (n = 10). *C*, neurological deficit scored at 24 h and 7 days after MCAO. *Ndrg4*$^{-/-}$ mice had a severe neurological deficit score compared with *Ndrg4*$^{+/+}$ mice. Data are mean ± S.D. (n = 10). *D*, rCBF in the penumbra-like peripheral area of the ischemic legion. The rCBF was measured by laser-Doppler blood flowmetry system. The rCBFs were expressed as percentages of their preischemic normal values. During MCAO, rCBF was reduced to an equivalent level, and reperfusion was achieved in both groups, although the rCBF values of *Ndrg4*$^{-/-}$ mice were lower compared with *Ndrg4*$^{+/+}$ mice. Data are mean with error bars of S.D. in *Ndrg4*$^{+/+}$ (○, n = 7) and *Ndrg4*$^{-/-}$ mice (●, n = 5). The differences in rCBF between *Ndrg4*$^{+/+}$ and *Ndrg4*$^{-/-}$ mice at each point were not significant.

rating the histological results, MCAO-treated *Ndrg4*$^{-/-}$ mice showed more severe neurological deficits compared with *Ndrg4*$^{+/+}$ mice in the cerebral function scoring test (Fig. 5*C*). At 7 days after the 15-min MCAO, the infarction volumes were significantly larger in *Ndrg4*$^{-/-}$ mice compared with *Ndrg4*$^{+/+}$ mice, as seen in the acute phase study (Fig. 5*B*). However, differences in neurological deficit scores between *Ndrg4*$^{+/+}$ and *Ndrg4*$^{-/-}$ mice decreased at the end of the observation period (Fig. 5*C*).

Physiological measures of *Ndrg4*$^{+/+}$ and *Ndrg4*$^{-/-}$ mice, heart rate (24 h, 477 ± 100 *versus* 464 ± 95 beat/min, n = 10; 7 days, 497 ± 57 *versus* 483 ± 131 beat/min, n = 7 and 5, respectively) and mean blood pressure (24 h, 46 ± 8 *versus* 55 ± 13 mm Hg, n = 10; 7 days, 68 ± 10 *versus* 63 ± 25 mm Hg, n = 7 and 5, respectively) were not significantly different during ischemic treatment. These results indicate that NDRG4 is essential for the acquisition of normal resistance to the acute and chronic phase of cerebral ischemia through the retention of BDNF levels.

rCBF—We monitored the rCBF in the penumbra-like peripheral area of the ischemic legion to exclude the possibility that the larger infarct in the *Ndrg4*$^{-/-}$ brain was due to a decrease of rCBF during MCAO. Using laser-Doppler blood flowmetry, we found that rCBF values during the 15-min MCAO were equivalently reduced in *Ndrg4*$^{+/+}$ (8.4 ± 3.2%) and *Ndrg4*$^{-/-}$ (7.1 ± 2.0%) mice (Fig. 5*D*). After MCAO, perfusion was observed in both groups as expected, but the rCBF values were relatively lower in *Ndrg4*$^{-/-}$ than in *Ndrg4*$^{+/+}$ mice, which indicates that the sensitivity to ischemic stress is increased under a deficiency of NDRG4.

DISCUSSION

In this study, we revealed that NDRG4 was involved in the retaining of BDNF levels in the cortex. We also revealed that NDRG4-deficient mice showed cognitive deficits and impaired cerebral infarction tolerance. Although these phenomena in the brain seem to be physiologically distinct from each other, the abilities in learning/memory and neuroprotection are both appropriate indicators of biological activities involving BDNF (20).

BDNF participates in synaptic plasticity and memory processing in the adult brain (22). Indeed, mice that lack BDNF in their forebrain fail to learn the MWM task (21), whereas an increase in BDNF levels in the brain improves spatial learning and memory (22, 26). These observations are consistent with our findings that *Ndrg4*$^{-/-}$ mice have lower amounts of cortex BDNF than *Ndrg4*$^{+/+}$ and impaired spatial learning and memory function. Because BDNF also increases the survivability of neurons against ischemia, decreased levels of BDNF in the *Ndrg4*$^{-/-}$ cortex can explain the enlarged lesion sizes that appeared after the stress induced by temporary focal ischemia (23–26). BDNF-mediated production of prostacyclin (36) may be associated with the neuronal vulnerabilities of the *Ndrg4*$^{-/-}$ mice because prostacyclin has a potent neuroprotective effect against focal cerebral ischemia (37). Despite the decreased levels of BDNF in the cortex of *Ndrg4*$^{-/-}$ mice, the neurological deficits were recovered at 7 days after ischemia. It needs further investigations to clarify the mechanisms of neurologic recovery in *Ndrg4*$^{-/-}$ mice. Some signaling pathways mediated by BDNF receptors such as tropomyosin-related kinase B might be up-regulated by a sustained decrease of BDNF in *Ndrg4*$^{-/-}$ mice.

The expression of NDRG4 is decreased in the brains of patients with Alzheimer's disease (15), and BDNF expression is also decreased in the cortex of Alzheimer's patients (22), observations consistent with our current finding of decreased levels of BDNF in the *Ndrg4*$^{-/-}$ mouse brain. Therefore, it is likely that NDRG4 exists upstream of the BDNF production. A decrease of NDRG4 may cause neuronal vulnerability via an associated reduction of BDNF levels and thus may be a potential contributor or a risk factor in the pathogenesis of Alzheimer's disease.

Although the molecular mechanisms by which NDRG4 influences cerebral BDNF levels are unknown, NDRG4-mediated signaling pathways may play an essential role in BDNF synthesis and secretion. BDNF secretion is dependent on the activation of voltage-gated Na^+ channels and the subsequent of Ca^{2+} influx through voltage-gated N-type Ca^{2+} channels (38). In addition, BDNF release is involved in caffeine/ryanodine-sensitive Ca^{2+} release from intracellular stores. These findings support the idea that NDRG4 might regulate BDNF secretion via Ca^{2+} mobilization.

In contrast to the dysfunctional effects of NDRG4 deficiency on the central nervous system, NDRG1 deficiency results in peripheral nervous system defects. Although a brain magnetic resonance imaging study demonstrated subcortical white matter abnormalities in sibling patients with Charcot-Marie-Tooth disease type 4D (39), the lack of NDRG1 exhibited no adverse effects on higher brain functions (9) and on brain anatomy (17), suggesting that other NDRG members may compensate for the NDRG1 deficiency in the central nervous system. Similarly, the mild phenotypes of the *Ndrg4*$^{-/-}$ mice may be due to the compensatory action of the other NDRG members. Further analysis using double-knockout mice such as *Ndrg1*$^{-/-}$*Ndrg4*$^{-/-}$ may reveal the overlapping roles of the NDRG members.

Although the NDRG4 mRNA is abundantly expressed in the human brain and heart (15, 16), Western blotting analysis in the present study could only detect the NDRG4 protein isoforms in the brain but not in the heart of the wild-type mice. This was probably due to the extremely low levels of NDRG4 protein in the heart. This unexpected finding may be caused by the low translational efficiency or the instability of NDRG4 mRNA in the heart. However, recent reports implicate biological roles of NDRG4 in the heart. The knockdown of NDRG4 during embryonic development in zebrafish results in phenotypes such as a hypoplastic heart with pericardial edema, a dilated atrium, looping defects, reduced circulation, and a slower heart rate with weaker contraction (40). Severe ventricular hypoplasia down-regulates NDRG4 expression in the mouse embryonic heart (16). These reports indicate that NDRG4 is necessary for the normal regulation of myocardial proliferation and cardiac growth during early cardiogenesis. In addition, human chromosome 16q21 near *NDRG4* was identified as the locus that influences QT interval duration (41, 42). Although we currently do not find any histological and functional abnormalities for the *Ndrg4*$^{-/-}$ heart, more detailed studies may reveal the roles of NDRG4 on cardiac function.

In conclusion, we found that NDRG4 has an essential role in retaining normal spatial learning and memory, in protecting cerebral neurons against severe ischemic stress, and in maintaining BDNF levels in the brain within the normal range. Although the mechanisms by which NDRG4 influences intracerebral BDNF levels are yet unidentified, the decreased level of cortical BDNF may induce impairments in the central nervous system of *Ndrg4*$^{-/-}$ mice. Further investigation of *Ndrg4*$^{-/-}$ mice, including brain vasculature characterization and neurogenesis, may provide insight into effective therapies for some central nervous system diseases, including Alzheimer's disease and ischemic stroke.

Acknowledgment—We thank Dr. Yuka Eura for experimental materials.

REFERENCES

1. Yao, L., Zhang, J., and Liu, X. (2008) *Acta Biochim. Biophys. Sin.* **40,** 625–635
2. Schilling, S. H., Hjelmeland, A. B., Radiloff, D. R., Liu, I. M., Wakeman, T. P., Fielhauer, J. R., Foster, E. H., Lathia, J. D., Rich, J. N., Wang, X. F., and Datto, M. B. (2009) *J. Biol. Chem.* **284,** 25160–25169
3. Wang, W., Li, Y., Li, Y., Hong, A., Wang, J., Lin, B., and Li, R. (2009) *Int. J. Cancer* **124,** 521–530
4. Kitowska, A., and Pawelczyk, T. (2010) *Acta Biochim. Pol.* **57,** 15–21
5. Melotte, V., Qu, X., Ongenaert, M., van Criekinge, W., de Bruïne, A. P., Baldwin, H. S., and van Engeland, M. (2010) *FASEB J.* **24,** 4153–4166
6. Kokame, K., Kato, H., and Miyata, T. (1996) *J. Biol. Chem.* **271,** 29659–29665
7. Taketomi, Y., Sunaga, K., Tanaka, S., Nakamura, M., Arata, S., Okuda, T., Moon, T. C., Chang, H. W., Sugimoto, Y., Kokame, K., Miyata, T., Murakami, M., and Kudo, I. (2007) *J. Immunol.* **178,** 7042–7053
8. Kalaydjieva, L., Gresham, D., Gooding, R., Heather, L., Baas, F., de Jonge, R., Blechschmidt, K., Angelicheva, D., Chandler, D., Worsley, P., Rosenthal, A., King, R. H., and Thomas, P. K. (2000) *Am. J. Hum. Genet.* **67,** 47–58
9. Okuda, T., Higashi, Y., Kokame, K., Tanaka, C., Kondoh, H., and Miyata, T. (2004) *Mol. Cell. Biol.* **24,** 3949–3956
10. Drögemüller, C., Becker, D., Kessler, B., Kemter, E., Tetens, J., Jurina, K., Jäderlund, K. H., Flagstad, A., Perloski, M., Lindblad-Toh, K., and Matiasek, K. (2010) *PLoS ONE* **5,** e11258
11. Takahashi, K., Yamada, M., Ohata, H., Momose, K., Higuchi, T., Honda, K., and Yamada, M. (2005) *Int. J. Neuropsychopharmacol.* **8,** 381–389
12. Boulkroun, S., Fay, M., Zennaro, M. C., Escoubet, B., Jaisser, F., Blot-Chabaud, M., Farman, N., and Courtois-Coutry, N. (2002) *J. Biol. Chem.* **277,** 31506–31515
13. Choi, S. C., Kim, K. D., Kim, J. T., Kim, J. W., Yoon, D. Y., Choe, Y. K., Chang, Y. S., Paik, S. G., and Lim, J. S. (2003) *FEBS Lett.* **553,** 413–418
14. Burchfield, J. G., Lennard, A. J., Narasimhan, S., Hughes, W. E., Wasinger, V. C., Corthals, G. L., Okuda, T., Kondoh, H., Biden, T. J., and Schmitz-Peiffer, C. (2004) *J. Biol. Chem.* **279,** 18623–18632
15. Zhou, R. H., Kokame, K., Tsukamoto, Y., Yutani, C., Kato, H., and Miyata, T. (2001) *Genomics* **73,** 86–97
16. Dupays, L., Kotecha, S., Angst, B., and Mohun, T. J. (2009) *Dev. Biol.* **333,** 121–131
17. Okuda, T., Kokame, K., and Miyata, T. (2008) *J. Histochem. Cytochem.* **56,** 175–182
18. Ohki, T., Hongo, S., Nakada, N., Maeda, A., and Takeda, M. (2002) *Brain Res. Dev. Brain Res.* **135,** 55–63
19. Nishimoto, S., Tawara, J., Toyoda, H., Kitamura, K., and Komurasaki, T. (2003) *Eur. J. Biochem.* **270,** 2521–2531
20. Mattson, M. P. (2008) *Ann. N.Y. Acad. Sci.* **1144,** 97–112
21. Gorski, J. A., Balogh, S. A., Wehner, J. M., and Jones, K. R. (2003) *Neuroscience* **121,** 341–354
22. Nagahara, A. H., Merrill, D. A., Coppola, G., Tsukada, S., Schroeder, B. E., Shaked, G. M., Wang, L., Blesch, A., Kim, A., Conner, J. M., Rockenstein, E., Chao, M. V., Koo, E. H., Geschwind, D., Masliah, E., Chiba, A. A., and Tuszynski, M. H. (2009) *Nat. Med.* **15,** 331–337
23. Schäbitz, W. R., Schwab, S., Spranger, M., and Hacke, W. (1997) *J. Cereb. Blood Flow Metab.* **17,** 500–506
24. Yanamoto, H., Nagata, I., Sakata, M., Zhang, Z., Tohnai, N., Sakai, H., and Kikuchi, H. (2000) *Brain Res.* **859,** 240–248
25. Endres, M., Fan, G., Hirt, L., Fujii, M., Matsushita, K., Liu, X., Jaenisch, R., and Moskowitz, M. A. (2000) *J. Cereb. Blood Flow. Metab.* **20,** 139–144
26. Yanamoto, H., Xue, J. H., Miyamoto, S., Nagata, I., Nakano, Y., Murao, K., and Kikuchi, H. (2004) *Brain Res.* **1019,** 178–188
27. Agarwala, K. L., Kokame, K., Kato, H., and Miyata, T. (2000) *Biochem. Biophys. Res. Commun.* **272,** 641–647
28. Takagi, T., Moribe, H., Kondoh, H., and Higashi, Y. (1998) *Development*

125, 21–31
29. Yagi, T., Nada, S., Watanabe, N., Tamemoto, H., Kohmura, N., Ikawa, Y., and Aizawa, S. (1993) *Anal. Biochem.* **214,** 77–86
30. Nagy, A., Rossant, J., Nagy, R., Abramow-Newerly, W., and Roder, J. C. (1993) *Proc. Natl. Acad. Sci. U.S.A.* **90,** 8424–8428
31. Kokame, K., Agarwala, K. L., Kato, H., and Miyata, T. (2000) *J. Biol. Chem.* **275,** 32846–32853
32. Nakajo, Y., Miyamoto, S., Nakano, Y., Xue, J. H., Hori, T., and Yanamoto, H. (2008) *Brain Res.* **1241,** 103–109
33. Morris, R. (1984) *J. Neurosci. Methods* **11,** 47–60
34. Yanamoto, H., Nagata, I., Niitsu, Y., Xue, J. H., Zhang, Z., and Kikuchi, H. (2003) *Exp. Neurol.* **182,** 261–274
35. Yanamoto, H., Nagata, I., Niitsu, Y., Zhang, Z., Xue, J. H., Sakai, N., and Kikuchi, H. (2001) *Stroke* **32,** 232–239
36. Santhanam, A. V., Smith, L. A., and Katusic, Z. S. (2010) *Stroke* **41,** 350–356
37. Lin, H., Lin, T. N., Cheung, W. M., Nian, G. M., Tseng, P. H., Chen, S. F., Chen, J. J., Shyue, S. K., Liou, J. Y., Wu, C. W., and Wu, K. K. (2002) *Circulation* **105,** 1962–1969
38. Kolarow, R., Brigadski, T., and Lessmann, V. (2007) *J. Neurosci.* **27,** 10350–10364
39. Echaniz-Laguna, A., Degos, B., Bonnet, C., Latour, P., Hamadouche, T., Lévy, N., and Leheup, B. (2007) *Neuromuscul. Disord.* **17,** 163–168
40. Qu, X., Jia, H., Garrity, D. M., Tompkins, K., Batts, L., Appel, B., Zhong, T. P., and Baldwin, H. S. (2008) *Dev. Biol.* **317,** 486–496
41. Newton-Cheh, C., Eijgelsheim, M., Rice, K. M., de Bakker, P. I., Yin, X., Estrada, K., Bis, J. C., Marciante, K., Rivadeneira, F., Noseworthy, P. A., Sotoodehnia, N., Smith, N. L., Rotter, J. I., Kors, J. A., Witteman, J. C., Hofman, A., Heckbert, S. R., O'Donnell, C. J., Uitterlinden, A. G., Psaty, B. M., Lumley, T., Larson, M. G., and Stricker, B. H. (2009) *Nat. Genet.* **41,** 399–406
42. Pfeufer, A., Sanna, S., Arking, D. E., Müller, M., Gateva, V., Fuchsberger, C., Ehret, G. B., Orrú, M., Pattaro, C., Köttgen, A., Perz, S., Usala, G., Barbalic, M., Li, M., Pütz, B., Scuteri, A., Prineas, R. J., Sinner, M. F., Gieger, C., Najjar, S. S., Kao, W. H., Mühleisen, T. W., Dei, M., Happle, C., Möhlenkamp, S., Crisponi, L., Erbel, R., Jöckel, K. H., Naitza, S., Steinbeck, G., Marroni, F., Hicks, A. A., Lakatta, E., Müller-Myhsok, B., Pramstaller, P. P., Wichmann, H. E., Schlessinger, D., Boerwinkle, E., Meitinger, T., Uda, M., Coresh, J., Kääb, S., Abecasis, G. R., and Chakravarti, A. (2009) *Nat. Genet.* **41,** 407–414

SUPPLEMENTAL DATA (Yamamoto *et al.*)

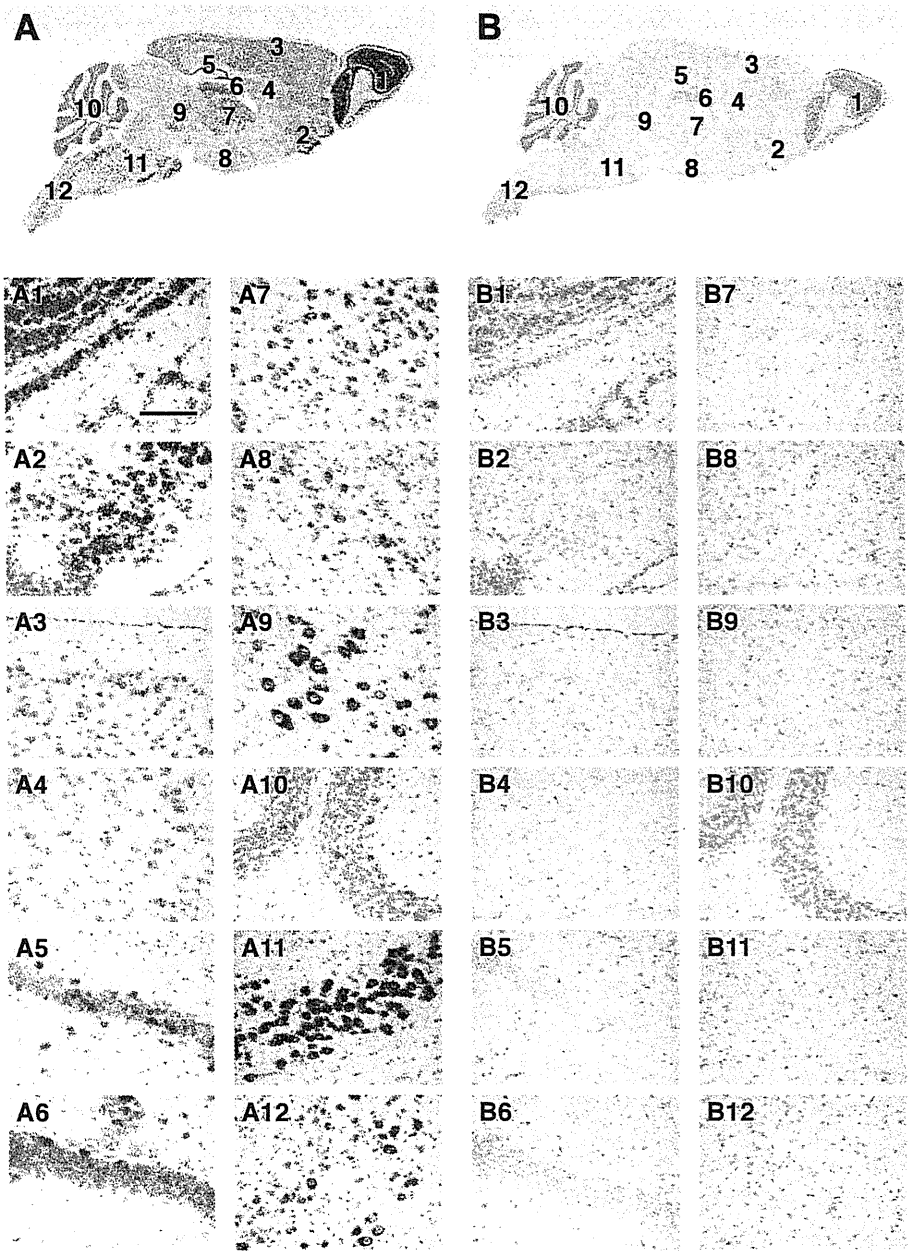

FIGURE S1. **Detailed localization of NDRG4 in the adult mouse brain.** Sagittal sections were prepared from 8-week-old wild-type mice and subjected to *in situ* mRNA hybridization of NDRG4. The DIG-labeled antisense riboprobes for NDRG4 (*A* and *A1–A12*), but not the sense riboprobes (*B* and *B1-B12*, negative control) produced positive signals shown in blue. The nuclei were counterstained in red with Kernechtrot stain solution. *A1–A12* and *B1–B12* are higher-magnification images of the numbered areas in *A* and *B*, respectively. *1*, olfactory bulb; *2*, olfactory tuberculum; *3*, cerebral cortex; *4*, striatum; *5*, hippocampus; *6*, dentate gyrus; *7*, thalamus; *8*, hypothalamus; *9*, mesencephalon; *10*, cerebellum; *11*, pons; *12*, medulla oblongata. *Bar*, 100 μm (for *A1–B12*).

Polymorphisms and mutations of *ADAMTS13* in the Japanese population and estimation of the number of patients with Upshaw–Schulman syndrome

K. KOKAME,* Y. KOKUBO† and T. MIYATA*
*Departments of *Molecular Pathogenesis and †Preventive Cardiology, National Cerebral and Cardiovascular Center, Suita, Osaka, Japan*

To cite this article: Kokame K, Kokubo Y, Miyata T. Polymorphisms and mutations of *ADAMTS13* in the Japanese population and estimation of the number of patients with Upshaw–Schulman syndrome. *J Thromb Haemost* 2011; **9**: 1654–6.

See also Kokame K, Sakata T, Kokubo Y, Miyata T. von Willebrand factor-to-ADAMTS13 ratio increases with age in a Japanese population. *J Thromb Haemost* 2011; **9**: 1426–8.

Upshaw–Schulman syndrome (USS), also called hereditary thrombotic thrombocytopenic purpura, is an autosomal recessive disease characterized by thrombocytopenia and microangiopathic hemolytic anemia. USS is associated with hereditary severe deficiency of plasma ADAMTS13 activity; patients with USS have homozygous or compound heterozygous mutations in the *ADAMTS13* gene [1–5]. ADAMTS13 is a plasma metalloprotease that regulates platelet aggregation through the cleavage of von Willebrand factor (VWF) multimers. ADAMTS13-deficient plasma derived from patients with USS contains unusually large VWF multimers, which can induce unwanted hyperaggregation of platelets and microvascular thrombi. In this study, we analyzed the relationship between genetic variation of *ADAMTS13* and plasma ADAMTS13 activity in the Japanese general population. In addition, on the basis of the data obtained via our genetic analysis, we estimated the number of patients with USS in Japan.

The population examined is based on the Suita Study [6], an epidemiologic study consisting of randomly selected Japanese residents of Suita City, which is located in the second largest urban area in Japan. Our study protocol was approved by the ethical review committee of the National Cerebral and Cardiovascular Center, and only subjects who provided written informed consent for genetic analyses were included.

To identify common polymorphisms in the population, we first sequenced all 29 exons and exon–intron boundaries of *ADAMTS13* using 346 consecutive subjects, by means of previously described methods [2]. We identified 25 polymorphisms with allele frequencies of the respective minor allele > 0.01, including two in the promoter region, 10 in the exons, and 13 in the introns. Of these, six were missense single-nucleotide polymorphisms (SNPs): p.T339R (c.1016C > G), p.Q448E (c.1342C > G), p.P475S (c.1423C > T), p.P618A (c.1852C > G), p.S903L (c.2708C > T), and p.G1181R (c.3541G > A). Next, we performed TaqMan genotyping assays (Applied Biosystems, Tokyo, Japan) for the missense SNPs, using 3616 subjects whose plasma ADAMTS13 activities had been measured with the FRETS-VWF73 assay [7]. Allele frequencies for the minor alleles were 0.027 for p.T339R, 0.192 for p.Q448E, 0.050 for p.P475S, 0.027 for p.P618A, 0.048 for p.S903L, and 0.022 for p.G1181R. The observed genotypes did not deviate significantly from Hardy–Weinberg equilibrium. The p.T339R and p.P618A SNPs were in absolute linkage disequilibrium (r^2 = 0.97), whereas the other missense SNPs were not strongly linked (r^2 < 0.11).

The p.Q448E and p.P475S SNPs, but not the other missense SNPs, were significantly associated with plasma ADAMTS13 activity (Fig. 1A). The ADAMTS13 activity (97% ± 25% in men, 111% ± 28% in women, mean ± standard deviation) of p.Q448E heterozygotes (QE) and minor allele homozygotes (EE) was slightly but significantly higher than that of major allele homozygotes (QQ) (91% ± 24% in men, 104% ± 26% in women). In contrast, the ADAMTS13 activity (79% ± 20% in men, 92% ± 24% in women) of p.P475S heterozygotes (PS) and minor allele homozygotes (SS) was significantly lower than that of major allele homozygotes (PP) (94% ± 24% in men, 108% ± 27% in women). The difference in activity was consistent with the observation that the recombinant ADAMTS13-P475S mutant has approximately 70% of the activity of wild-type ADAMTS13 [8]. It is interesting that p.P618A was not associated with plasma ADAMTS13 activity in the present study, whereas the conditioned medium of HEK293 cells expressing the A618 variant showed lower levels of activity (27%) and antigen (14%) than the wild type [9]. PolyPhen-2, a program that predicts damaging missense mutations [10], identified p.T339R and p.P618A as 'possibly damaging' and 'probably damaging', respectively, whereas the other four SNPs were predicted to be 'benign'.

As the *ADAMTS13* locus is near (130–190 kb) the *ABO* locus on chromosome 9q34, we compared the frequencies of the SNPs among ABO blood group genotypes (Fig. 1B). The relative frequencies of p.T339R minor allele homozygotes and

Correspondence: Koichi Kokame, PhD, Department of Molecular Pathogenesis, National Cerebral and Cardiovascular Center, 5-7-1 Fujishirodai, Suita, Osaka 565-8565, Japan.
Tel.: +81 6 6833 5012; fax: +81 6 6835 1176.
E-mail: kame@ri.ncvc.go.jp

DOI: 10.1111/j.1538-7836.2011.04399.x

Received 30 March 2011, accepted 6 June 2011

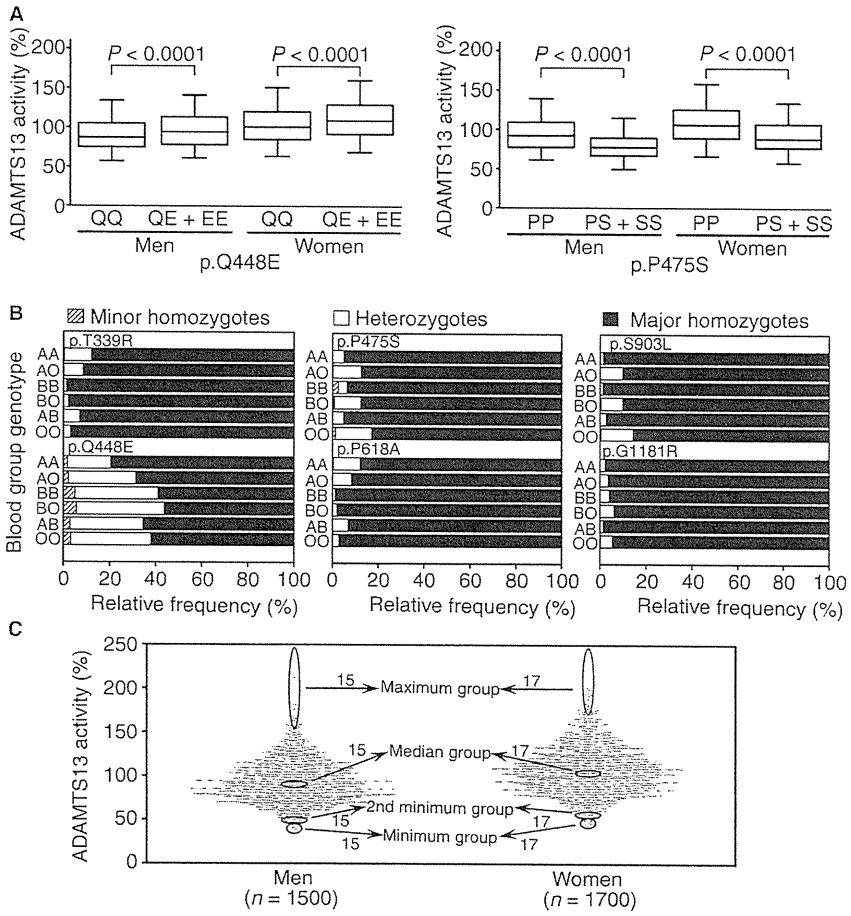

D

		Min. (n = 32)	2nd min. (n = 32)	Med (n = 32)	Max. (n = 32)
Average activity		47.1%	53.1%	97.6%	183%
Common SNP	p.T339R	2	1	3	0
	p.Q448E	8 (1)	8	8	16
	p.P475S	9 (2)	6	2	1
	p.P618A	2	1	3	0
	p.S903L	2	3	5	3
	p.G1181R	2	4	1	1
Rare mutation		7	3	2	2

Fig. 1. *ADAMTS13* variation in a Japanese general population. (A) Box-and-whisker plot (5th–95th percentiles) of plasma ADAMTS13 activity in each genotype of p.Q448E and p.P475S. *P*, Kruskal–Wallis test. (B) The relative frequency of minor homozygotes, heterozygotes and major homozygotes for each genetic polymorphism. (C) Scatter dot plot of plasma ADAMTS13 activity for men and women. On the basis of these activity measurements, 128 subjects were selected for sequencing of *ADAMTS13*. (D) The numbers of minor allele carriers in each group. One in eight p.Q448E carriers and two in nine p.P475S carriers in the minimum group were homozygotes for the respective minor alleles.

heterozygotes were higher for AA, AO and AB than for BB, BO and OO, suggesting that p.T339R is associated with the blood group A allele. The p.P618A SNP, which is tightly associated with p.T339R, exhibited the same pattern. The p.P475S and p.S903L SNPs tended to be associated with the blood group O allele.

We then utilized the plasma ADAMTS13 activity data to estimate the frequency of hereditary ADAMTS13 deficiency. In the population, 3200 DNA samples (1500 men and 1700 women) were available, from a quantitative standpoint, for sequencing of *ADAMTS13*. We selected 128 subjects according to their plasma ADAMTS13 activity (Fig. 1C): 32 subjects of the 'minimum' group (average activity, 47.1%), consisting of 15 men and 17 women with the lowest activities in each gender; 32 subjects of the 'second minimum' group (53.1%), consisting of 15 men and 17 women with the second lowest activities; 32 subjects of the 'median' group (97.6%), consisting of 15 men and 17 women with median activities; and 32 subjects of the 'maximum' group (183%), consisting of 15 men and 17 women with the highest activities. Each group corresponds to 1% of the population examined. All DNA samples from the four groups were subjected to *ADAMTS13* sequencing, which

revealed that 70 individuals had at least one of the six missense SNPs described above (Fig. 1D). Of these, only p.P475S showed a significant difference in minor allele frequency among four groups (P = 0.028, chi-square test). In addition, 14 individuals had rare non-synonymous mutations: seven (p.F324L, p.F418L, p.I673F, p.Q773X, p.Y1074AfsX46, p.R1095Q, and p.S1314L) in the 'minimum' group; three (p.I380T, p.Y1074AfsX46, and p.R1274C) in the 'second minimum' group; two (p.Q723K and p.N1321S) in the 'median' group; and two (p.L19F and p.R268Q) in the 'maximum' group. Of these, p.I673F (c.2017A > T) and p.Y1074AfsX46 (c.3220delTACC) had been identified as causative mutations in patients with USS [11,12]. All of the others were newly identified mutations.

To estimate the number of individuals with a hereditary ADAMTS13 deficiency, we generated several hypotheses: (i) as two individuals in each of the 'median' and 'maximum' groups had rare mutations, two of every 32 people should have a mutation that does not cause a functional defect of ADAMTS13; (ii) thus, five (= 7 − 2) individuals in the 'minimum' group and one (= 3 − 2) individual in the 'second minimum' group should be the heterozygotes carrying a mutation with a functional defect; (iii) other than these six (= 5 + 1) individuals in the 'minimum' and 'second minimum' groups, no individual should have any mutations that confer a functional defect. These hypotheses were consistent with a prediction based on PolyPhen-2: the p.S1314L, p.I380T, p.Q723K, p.N1321S, p.L19F and p.R268Q mutations are 'benign', p.I673F and p.R1274C are 'possibly damaging', and the others are 'probably damaging'. According to the hypotheses, we estimated that six of 3200 individuals were heterozygotes for ADAMTS13 deficiency. This estimation suggested that ~ 1 individual in 1.1×10^6 (= 6/3200 × 6/3200 × 1/4) should be a homozygote or a compound heterozygote for ADAMTS13 deficiency. In Japan, which has a population of approximately 1.3×10^8, ~ 110 individuals may have hereditary ADAMTS13 deficiency or USS. If we adjusted our estimate of ADAMTS13 deficiency from 6/3200 to 7/3200 or 5/3200, the number of patients would be 160 or 80, respectively. The validity of these calculation procedures was confirmed by StaGen Co., Ltd (Chiba, Japan), a company specializing in genetics, statistics, and data analysis.

In conclusion, this study demonstrated that, in the Japanese general population, there are six common missense SNPs: p.T339R, p.Q448E, p.P475S, p.P618A, p.S903L, and p.G1181R. Of these, p.Q448E and p.P475S are significantly associated with plasma ADAMTS13 activity. Allele frequencies of these SNPs correlate with ABO blood group. Finally, we estimated the number of patients with USS in Japan, yielding a figure that corresponds to approximately three times the number of patients already diagnosed as having this condition. Because of insufficient sample sizes, we may have underestimated the prevalence of USS. Further studies are needed to obtain more reliable conclusions.

Acknowledgements

This work was supported by grants-in-aid from the Ministry of Health, Labour, and Welfare of Japan, from the Ministry of Education, Culture, Sports, Science and Technology of Japan, and from the Program for Promotion of Fundamental Studies in Health Sciences of the National Institute of Biomedical Innovation (NIBIO) of Japan.

Disclosure of Conflict of Interests

The authors state that they have no conflict of interest.

References

1 Levy GG, Nichols WC, Lian EC, Foroud T, McClintick JN, McGee BM, Yang AY, Siemieniak DR, Stark KR, Gruppo R, Sarode R, Shurin SB, Chandrasekaran V, Stabler SP, Sabio H, Bouhassira EE, Upshaw JD Jr, Ginsburg D, Tsai HM. Mutations in a member of the *ADAMTS* gene family cause thrombotic thrombocytopenic purpura. *Nature* 2001; **413**: 488–94.

2 Kokame K, Matsumoto M, Soejima K, Yagi H, Ishizashi H, Funato M, Tamai H, Konno M, Kamide K, Kawano Y, Miyata T, Fujimura Y. Mutations and common polymorphisms in *ADAMTS13* gene responsible for von Willebrand factor-cleaving protease activity. *Proc Natl Acad Sci USA* 2002; **99**: 11902–7.

3 Moake JL. Thrombotic thrombocytopenic purpura: survival by 'giving a dam'. *Trans Am Clin Climatol Assoc* 2004; **115**: 201–19.

4 Sadler JE. von Willebrand factor, ADAMTS13, and thrombotic thrombocytopenic purpura. *Blood* 2008; **112**: 11–18.

5 Lotta LA, Garagiola I, Palla R, Cairo A, Peyvandi F. *ADAMTS13* mutations and polymorphisms in congenital thrombotic thrombocytopenic purpura. *Hum Mutat* 2010; **31**: 11–19.

6 Kokubo Y, Kamide K, Okamura T, Watanabe M, Higashiyama A, Kawanishi K, Okayama A, Kawano Y. Impact of high-normal blood pressure on the risk of cardiovascular disease in a Japanese urban cohort: the Suita study. *Hypertension* 2008; **52**: 652–9.

7 Kokame K, Sakata T, Kokubo Y, Miyata T. von Willebrand factor-to-ADAMTS13 ratio increases with age in a Japanese population. *J Thromb Haemost* 2011; **9**: 1426–8.

8 Akiyama M, Kokame K, Miyata T. ADAMTS13 P475S polymorphism causes a lowered enzymatic activity and urea lability in vitro. *J Thromb Haemost* 2008; **6**: 1830–2.

9 Plaimauer B, Fuhrmann J, Mohr G, Wernhart W, Bruno K, Ferrari S, Konetschny C, Antoine G, Rieger M, Scheiflinger F. Modulation of ADAMTS13 secretion and specific activity by a combination of common amino acid polymorphisms and a missense mutation. *Blood* 2006; **107**: 118–25.

10 Adzhubei IA, Schmidt S, Peshkin L, Ramensky VE, Gerasimova A, Bork P, Kondrashov AS, Sunyaev SR. A method and server for predicting damaging missense mutations. *Nat Methods* 2010; **7**: 248–9.

11 Matsumoto M, Kokame K, Soejima K, Miura M, Hayashi S, Fujii Y, Iwai A, Ito E, Tsuji Y, Takeda-Shitaka M, Iwadate M, Umeyama H, Yagi H, Ishizashi H, Banno F, Nakagaki T, Miyata T, Fujimura Y. Molecular characterization of *ADAMTS13* gene mutations in Japanese patients with Upshaw–Schulman syndrome. *Blood* 2004; **103**: 1305–10.

12 Fujimura Y, Matsumoto M, Kokame K, Soejima K, Murata M, Miyata T. Natural history of Upshaw–Schulman syndrome based on *ADAMTS13* gene analysis. *J Thromb Haemost In press*.